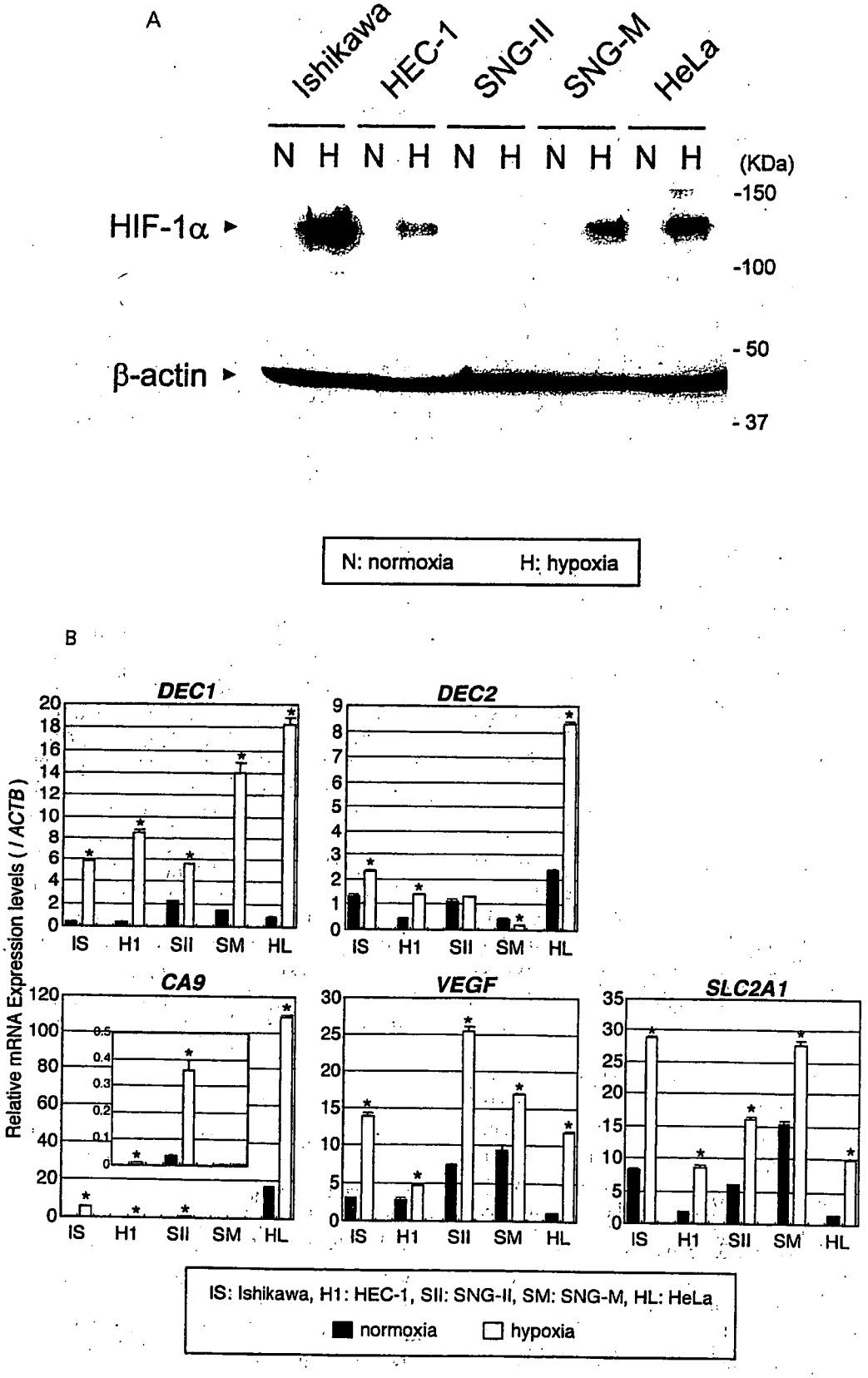

Figure 1. Activation of the HIF-1 pathway in the endometrial carcinoma cell lines. (A) The hypoxic induction of the HIF-1α protein. HIF-1α protein levels were evaluated under normoxic or hypoxic conditions in 4 human endometrial carcinoma cell lines by immunoblot analysis. After incubation under normoxic (21% pO_2) or hypoxic (1% pO_2) conditions for 12 h, the cells were harvested and whole cell extracts were prepared. HeLa, a cervical carcinoma cell line, was used as a positive control for the HIF-1α induction. (B) The hypoxic inductions of *DEC1* and *DEC2*, as well as known hypoxia-inducible gene expressions. The cancer cell lines were incubated under the same hypoxic conditions as above, and then total RNAs were extracted from the cell pellets. Real-time RT-PCR analyses of 5 HIF-1 target genes were performed, and the relative gene expression levels were calculated as the ratio to the expression level of *ACTB* (ß-actin). A cDNA mix, consisting of 17 various cell lines, was used to create standard curve of gene expression. Each value represents the mean ± SD for at least three independent experiments. The *P*-values were calculated using the Student's *t*-test. **P*<0.001.

Table II. Summary of the immunohistochemical analysis of the HIF-1α expression.

All	HIF-1α expression status			
	Negative	Positive		
n (%)		N>T	N=T	N<T
37 (100)	5 (13.5)	0 (0)	5 (13.5)	27 (73)

N, normal; T, tumor.

We then analyzed the expressions of 5 HIF-1 target genes, *DEC1*, *DEC2*, *CA9*, *VEGF*, and *SLC2A1*, in endometrial carcinomas, atypical hyperplasias, and adjacent normal endometria, in order to clarify the significance of these genes in carcinogenesis (Fig. 3). The expression level of each gene was determined as the mean value of the triplicated real-time RT-PCR analyses for comparison in the 3 tissue groups: Eighty-two endometrial carcinomas, 21 adjacent normal endometria, and 4 complex atypical endometrial hyperplasias. Although there was no significant difference in the expression levels of *DEC1* and *VEGF* among the 3 groups, the expression levels of the other 3 genes, *DEC2*, *CA9*, and *SLC2A1*, were found to be higher in atypical hyperplasia (P=0.026, P<0.004 and P<0.005) and carcinoma tissues (P=0.0024, P<0.0001 and P<0.0001), compared with those in normal tissues. Although there was no significant difference in the expression levels in the atypical hyperplasia and carcinoma samples, increases in the expression of the 3 genes likely correlated with the carcinogenesis of endometrial tissues.

Clinicopathological analyses of hypoxia-inducible gene expression in endometrial carcinomas. Lastly, we investigated the association between the hypoxia-inducible gene expression and the clinicopathological features in 82 endometrial carcinomas (Table III). The association analysis revealed that all 4 genes, except *DEC1*, were related to some of the clinicopathological features of tumors: The *DEC1* expression did not relate to any of the clinicopathological features. However, the *DEC2* expression levels were likely associated with the FIGO grade (P=0.052); the high expression of *CA9* and *VEGF* significantly correlated with the menopausal status of patients; the expression of *VEGF* and *SLC2A1* was related to lymphatic involvement and lymph node metastasis; and the *SLC2A1* expression was also related to the FIGO stage. The mode of action of each HIF-1 target gene was discrete in the endometrial carcinomas, and the functions of *CA9*, *VEGF*, and *SLC2A1* in the carcinomas, overlapped in part.

Discussion

We have demonstrated here that hypoxia caused an increase in HIF-1α protein expression in 4 endometrial carcinoma cell lines, and that its 5 target genes - *DEC1*, *DEC2*, *CA9*, *VEGF*, and *SLC2A1* - also reactively increased in most of the cell

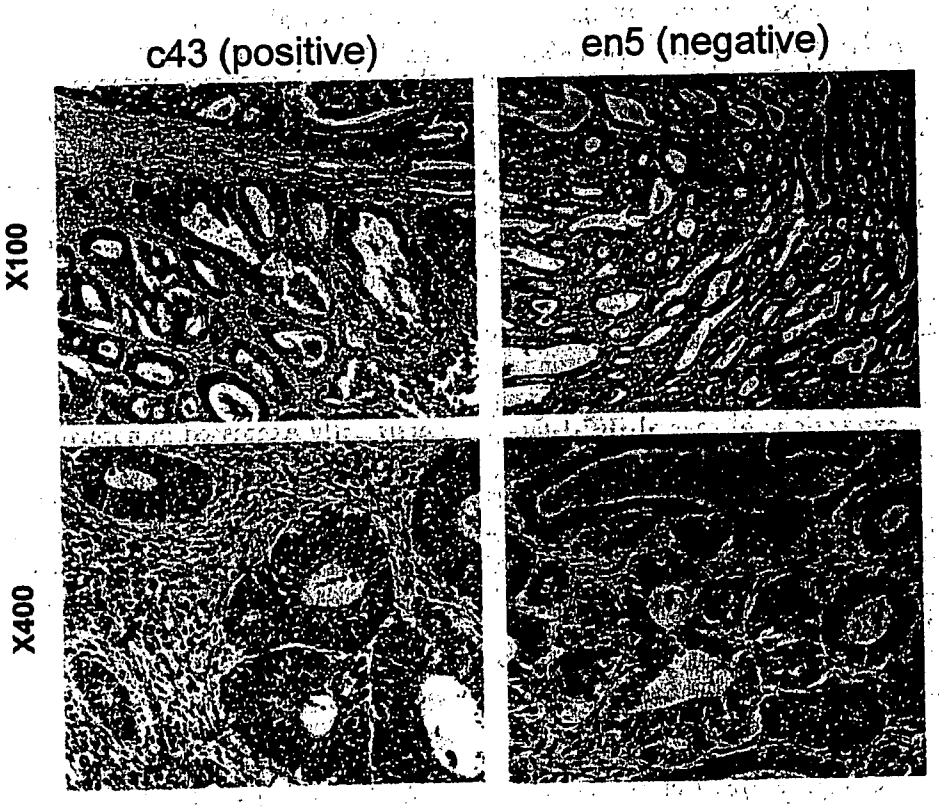

Figure 2. The expressions of the HIF-1α protein in endometrial carcinoma tissues. Representative examples of positive and negative staining for the HIF-1α protein were taken at x100 or x400 magnification. Immunoreactivity to HIF-1α was observed in the cytoplasm and nucleus of the cancer cells.

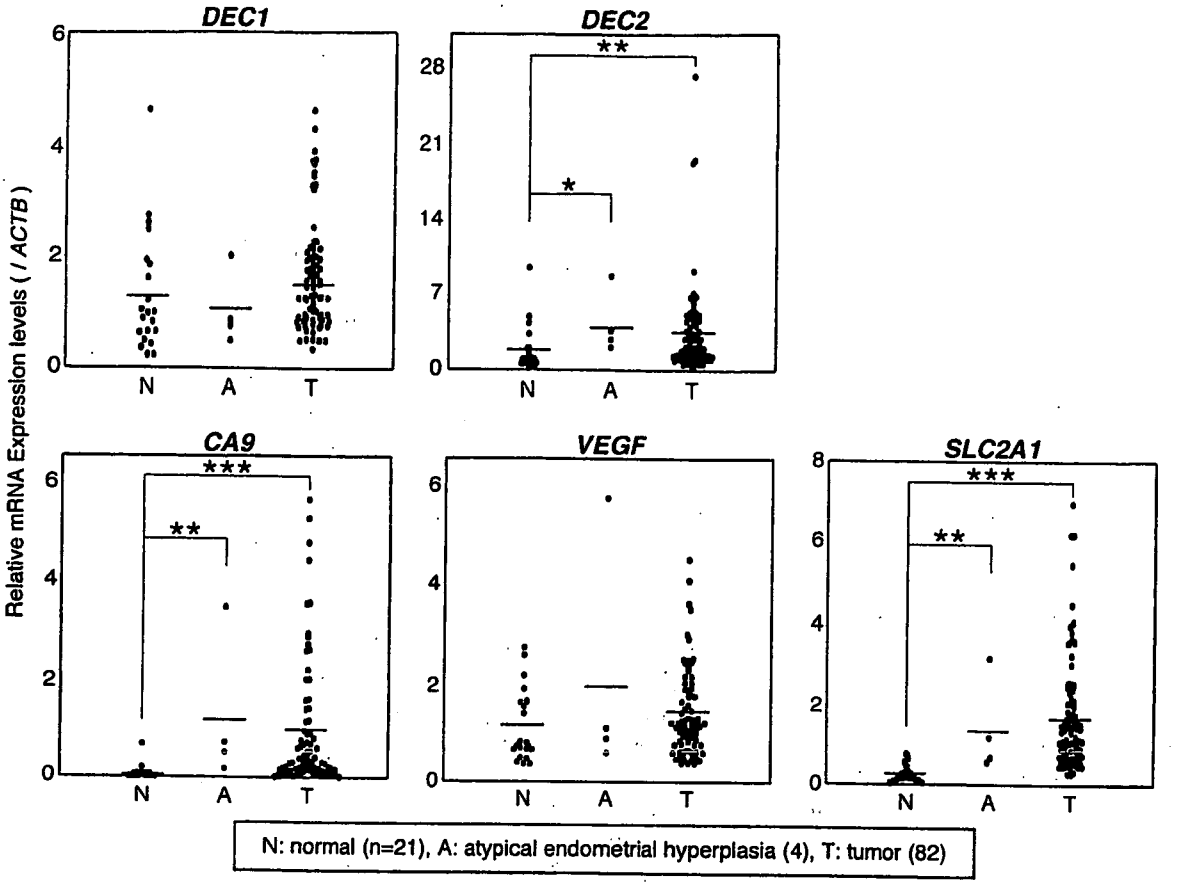

Figure 3. The expressions of hypoxia-inducible genes in normal, complex atypical endometrial hyperplasia, and endometrial carcinoma tissues. The expression levels of the 5 HIF-1 target genes were determined as the mean values of the triplicated real-time RT-PCR analyses for comparison in the 3 tissue groups: Eighty-two endometrial carcinomas, 21 adjacent normal endometria, and 4 complex atypical endometrial hyperplasias. The *P*-values were calculated using the Mann-Whitney *U* test. $^{*}P<0.05$, $^{**}P<0.005$, $^{***}P<0.0001$.

lines, except for *DEC2* in the SNG-M cells. We found that the expressions of *DEC2*, *CA9*, and *SLC2A1* were higher in complex atypical endometrial hyperplasia and endometrial carcinoma tissues compared with those in normal endometria. Furthermore, although the immunolabeling index of the HIF-1α protein in the carcinoma tissues did not correlate with any clinicopathological features of the tumors, the expression of 2 HIF-1 target genes correlated with aggressive clinicopathological features in 82 endometrial carcinomas: *VEGF* and/or *SLC2A1* correlated with lymphatic involvement, lymph-node metastasis, and the FIGO stage, and *CA9* and *VEGF*, correlated with the menopausal status, suggesting the existence of cross-talk between hypoxia- and estrogen-signaling. Since the expressions of several HIF-1-target genes increased in the process of endometrial carcinogenesis and were related to clinicopathological characteristics, it is likely that the activation of the HIF-1 pathway could play a key role in carcinogenesis and tumor phenotype development in endometrial carcinoma. However, only *DEC2* inversely correlated with the FIGO grade in its expression level.

DEC2 is involved in tissue development and regulation of the circadian rhythm as a transcriptional repressor (11,14,15), although its specific function in cancer remains to be clarified. Several reports have commented on the role of the other HIF-1 target genes including *DEC1* in various cancers (16-19), and GLUT1 (*SLC2A1* product) in endometrioid adenocarcinomas (23). However, ours is the first report to analyze the roles of *DEC2* in endometrial carcinoma. Our data suggest that *DEC2* can act on carcinogenesis and tumor phenotype development independently of the other HIF-1 target genes including *DEC1*. It should be noted that, among the various genes, differences between *DEC1* and *DEC2* were noticeable: Contrary to the unchanged *DEC1* expression, *DEC2* increased its expression levels in atypical hyperplasia or endometrial carcinoma compared to normal endometria, suggesting an association with carcinogenesis. The *DEC1* protein expression analyses in lung or breast cancers (16-18), revealed an augmented expression in breast cancers. Although the *DEC1* protein expression was observed in 38% in a series of 115 non-small cell lung carcinomas, *DEC1* was persistently expressed in normal bronchial and alveolar tissues, suggesting that the loss of *DEC1* expression could be an early event in the development of lung cancer (19). Furthermore, it has been demonstrated that the *DEC1/2* distribution in the organs is different (11). Despite some inconsistent data, the overall reactivity of *DEC2* to hypoxia correlated with that of the HIF-1α protein *in vitro*, possibly suggesting its distinctive nature, i.e., HIF-1-dependent induction. Although *DEC2* promotes carcinogenesis, as opposed to *DEC1* in lung cancers, their functions in carcinomas could be origin- or cell type-specific and thereby discrete. The *DEC2* expression in cancer cell lines could be determined by certain *DEC2*-targeting mechanisms that occur during carcinogenesis. Despite an incomplete under-

Table III. Statistical analysis of the clinicopathological characteristics relative to gene expression levels in endometrial carcinomas.

	Mean of relative expression/ACTB P-value														
Variables (n)	*DEC1*	*t*	*U*	*DEC2*	*t*	*U*	*CA9*	*t*	*U*	*VEGF*	*t*	*U*	*SLC2A1*	*t*	*U*
Menopausal status															
Pre (36)	1.507	0.470	0.266	3.669	0.632	0.550	0.677	0.167	**0.030**	1.137	**0.008**	**<0.001**	1.783	0.853	0.575
Post (46)	1.667			3.217			1.074			1.663			1.724		
Histological subtype															
Endometrioid (77)	1.632	0.349	0.410	3.208	0.079	0.337	0.928	0.437	0.568	1.391	0.106	0.094	1.770	0.620	0.720
Non-endometrioid (5)	1.195			6.610			0.463			2.065			1.444		
FIGO grade															
1 or 2 (61)	1.634	0.711	0.739	3.621	0.184	**0.052**	1.014	0.432	0.414	1.294	0.060	0.280	1.709	0.348	0.200
3 (7)	1.478			1.466			0.581			1.984			2.265		
MI															
<50% (63)	1.638	0.492	0.746	3.314	0.694	0.478	0.859	0.607	0.513	1.395	0.500	0.499	1.685	0.452	0.520
≥50% (19)	1.459			3.751			1.034			1.555			1.966		
LVI															
Absent (37)	1.453	0.233	0.137	3.069	0.503	0.140	0.971	0.650	0.246	1.226	0.060	**0.026**	1.270	**0.005**	**0.017**
Present (45)	1.715			3.699			0.841			1.602			2.145		
LN status															
Negative (61)	1.580	0.753	0.363	3.555	0.295	0.390	0.872	0.679	0.987	1.280	**0.011**	0.072	1.506	**0.001**	0.067
Positive (10)	1.690			2.101			0.687			2.038			3.057		
FIGO stage															
I or II (63)	1.629	0.592	0.987	3.686	0.290	0.359	0.947	0.549	0.672	1.363	0.210	0.145	1.557	**0.024**	0.178
III or IV (19)	1.490			2.517			0.743			1.661			2.389		
Recurrence status															
Negative (74)	1.623	0.462	0.815	3.293	0.428	0.827	0.947	0.311	0.553	1.387	0.175	0.195	1.730	0.703	0.719
Positive (8)	1.351			4.542			0.459			1.845			1.933		
Survival															
Surviving (78)	1.591	0.831	0.333	3.292	0.242	0.813	0.927	0.403	0.518	1.405	0.224	0.533	1.718	0.362	0.426
Deceased (4)	1.700			5.822			0.372			1.969			2.383		

t, Student's *t*-test; *U*, Mann-Whitney *U* test. Bold text, statistically significant.

standing of their functions as transcription repressors, findings that the expression of *DEC2* was stable in SNG-II, and further decreased in SNG-M under hypoxic conditions, could be explained by mutation(s) of the promoter region or the over-expression of transcriptional repressors such as *DEC1* (14).

We encountered unexpected data in our study: The activation of the HIF-1 downstream gene did not always correlate with the HIF-1α protein levels *in vitro*, and the immunolabeling index of the HIF-1α protein in carcinoma tissues did not correlate with any clinicopathological features of the tumors, contrary to the findings with the activated HIF-1 downstream genes *in vivo*. One hypothesis is that the HIF-1 pathway can be activated not only by hypoxia but also by the inactivation of several tumor suppressor genes such as *VHL*, *TP53* and *PTEN*, as reported elsewhere (5-7,26-28). Since mutations of *TP53* and *PTEN* were commonly observed in endometrial carcinomas, the inactivation of these tumor suppressor genes could be one of the mechanisms that activated the HIF-1 pathway in endometrial carcinogenesis (2,3). Our immnohistochemical analysis supported this hypothesis, since we found only nuclear staining in some adjacent stromal tissues, but both nuclear and cytoplasmic strong staining in the cancer cells, suggesting the aberrant activation of HIF-1α in cancer cells. The poor correlation in the activation between HIF-1α and its downstream genes could also be due to the involvement of the recruitment of coactivators and/or other transcription factors, including HIF-2α, among the mechanisms. Even so, the detailed mechanisms in the HIF-1 pathway activation and subsequently

in the carcinogenesis of endometrial carcinoma, as well as the functional roles of the HIF-1 downstream genes, remain unclear as with other cancers. Further investigation is required.

In conclusion, we demonstrated the increased expression of several hypoxia-inducible genes, including the previously unreported *DEC2* in endometrial carcinogenesis. The activation of the HIF-1 pathway played a part in carcinogenesis and tumor phenotype development in endometrial carcinoma. Among the HIF-1-target genes, the *DEC2* expression can be differentially regulated and plays a unique role in endometrial carcinogenesis.

Acknowledgements

We thank Dr Kouji Arihiro for the preparation of the tissue sections. We also thank Ms. H. Tagawa, Ms. C. Oda, Ms. K. Nukata, Ms. M. Wada, Ms. I. Fukuba, and Ms. M. Sasaki for their technical and secretarial support. A part of this study was carried out at the Analysis Center of Life Science, Hiroshima University, Japan.

References

1. Amant F, Moerman P, Neven P, Timmerman D, Van Limbergen E and Vergote I: Endometrial cancer. Lancet 366: 491-505, 2005.
2. Prat J: Prognostic parameter of endometrial carcinoma. Hum Pathol 35: 649-662, 2004.
3. Shiozawa T and Konishi I: Early endometrial carcinoma: clinicopathology, hormonal aspects, molecular genetics, diagnosis, and treatment. Int J Clin Oncol 11: 13-21, 2006.
4. Vaupel P, Kallinowski F and Okunieff P: Blood flow, oxygen and nutrient supply, and metabolic microenvironment of human tumors (Review). Cancer Res 49: 6449-6465, 1989.
5. Semenza GL: Targeting HIF-1 for cancer therapy. Nature Rev 3: 721-732, 2003.
6. Kondoh-Kizaka S, Inoue M, Harada H and Hiraoka M: Tumor hypoxia: A target for selective cancer therapy. Cancer Sci 94: 1021-1028, 2003.
7. Poellinger L and Johnson RS: HIF-1 and hypoxic response: the plot thickens. Curr Opin Genet Dev 14: 81-85, 2004.
8. Fandrey J, Gorr TA and Gassmann M: Regulating cellular oxygen sensing by hydroxylation. Cardiovasc Res (in press).
9. Miyazaki K, Kawamoto T, Tanimoto K, Nishiyama M, Honda H and Kato Y: Identification of functional hypoxia response elements in the promoter region of the DEC1 and DEC2 genes. J Biol Chem 277: 47014-47021, 2002.
10. Shen M, Kawamoto T, Teramoto M, Makihira S, Fujimoto K, Yan W, Noshiro M and Kato Y: Induction of basic helix-loop-helix protein DEC1 (BHLHB2)/Stra13/Sharp2 in response to the cyclic adenosine monophosphate pathway. Eur J Cell Biol 80: 329-334, 2001.
11. Fujimoto K, Shen M, Noshiro M, Matsubara K, Shingu S, Honda K, Yoshida E, Suardita K, Matsuda Y and Kato Y: Molecular cloning and characterization of DEC2, a new member of basic helix-loop-helix proteins. Biochem Biophys Res Commun 280: 164-171, 2001.
12. Shen M, Yoshida E, Yan W, Kawamoto T, Suardita K, Koyano Y, Fujimoto K, Noshiro M and Kato Y: Basic Helix-loop-Helix protein DEC1 promotes Chondrocyte differenciation at the early and terminal stages. J Biochem Chem 51: 50112-50120, 2002.
13. Yun Z, Maecker HL, Johonson RS and Giaccia AJ: Inhibition of PPAR gamma 2 gene expression by the HIF-1-regulated gene DEC1/Stra13: a mechanism for regulation of adipogenesis by hypoxia. Dev Cell 3: 331-341, 2002.
14. Hamaguchi H, Fujimoto K, Kawamoto T, Noshiro M, Maemura K, Takeda N, Nagai R, Furukawa M, Honma S, Honma K, Kurihara H and Kato Y: Expression of the gene for Dec2, a basic helix-loop-helix transcription factor, is regulated by a molecular clock system. Biochem J 382: 43-50, 2004.
15. Honma S, Kawamoto T, Takagi Y, Fujimoto K, Sato F, Noshiro M, Kato Y and Honma K: Dec1 and Dec2 are regulators of the mammalian molecular clock. Nature 419: 841-844, 2002.
16. Chakrabarti J, Turley H, Campo L, Han C, Harris AL, Gatter KC and Fox SB: The transcription factor DEC1 (stra13, SHARP2) is associated with the hypoxic response and high tumour grade in human breast cancers. Br J Cancer 91: 954-958, 2004.
17. Currie MJ, Hanrahan V, Gunningham SP, Morrin HR, Frampton C, Han C, Robinson BA and Fox SB: Expression of vascular endothelial growth factor D is associated with hypoxia inducible factor (HIF-1α) and HIF-1alpha target gene DEC1, but not lymph node metastasis in primary human breast carcinomas. J Clin Pathol 57: 829-834, 2004.
18. Turley H, Wykoff CC, Troup S, Watson PH, Gatter KC and Harris AL: The hypoxia-regulated transcription factor DEC1 (Stra13, SHARP-2) and its expression in human tissues and tumors. J Pathol 203: 808-813, 2004.
19. Giatromanolaki A, Koukourakis MI, Sivridis E, Turley H, Wykoff CC, Gatter KC and Harris AL: DEC1 (STRA13) protein expression relates to hypoxia-inducible factor 1-alpha and carbonic anhydrase-9 overexpression in non-small cell lung cancer. J Pathol 200: 222-228, 2003.
20. Robertson N, Potter C and Harris AL: Role of carbonic anhydrase IX in human tumor cell growth, survival, and invasion: Cancer Res 64: 61610-6165, 2004.
21. Acs G, Zhang PJ, McGrath CM, Acs P, McBroom J, Mohyeldin A, Liu S, Lu H and Verma A: Hypoxia-inducible erythropoietin signaling in squamous dysplasia and squamous cell carcinoma of the uterine cervix and its potential role in cervical carcinogenesis and tumor progression. Am J Pathol 162: 1789-1806, 2003.
22. Airley RE, Loncaster J, Raleigh JA, Harris AL, Davidson SE, Hunter RD, West CM and Stratford IJ: GLUT-1 and CAIX as intrinsic markers of hypoxia in carcinoma of the cervix: relationship to pimonidazole binding. Int J Cancer 104: 85-91, 2003.
23. Wang BY, Kalir T, Sabo E, Sherman DE, Cohen C and Burstein DE: Immunohistchemical staining of GLUT1 in benign, hyperplastic, and malignant endometrial epithelia. Cancer 88: 2772-2781, 2000.
24. Nisahida M: The Ishikawa cells from birth to the present. Hum Cell 15: 104-117, 2002.
25. Kallio PJ, Pongratz I, Gradin K, McGuire J and Poellinger L: Activation of hypoxia-inducible factor-1α: posttranscriptional regulation and conformational change by recruitment of the Arnt transcription factor. Proc Natl Acad Sci USA 94: 5667-5672, 1997.
26. Tanimoto K, Makino Y, Pereira T and Poellinger L: Mechanism of regulation of the hypoxia-inducible factor-1α by the von Hippel-Lindau tumor suppressor protein. EMBO J 19: 4298-4309, 2000.
27. Ravi R, Mookerjee B, Bhujwalla ZM, Sutter CH, Artemov D, Zeng Q, Dillehay LE, Madan A, Semenza GL and Bedi A: Regulation of tumor angiogenesis by p53-induced degradation of hypoxia-inducible factor 1α. Genes Dev 14: 34-44, 2000.
28. Zundel W, Schindler C, Haas-Kogan D, Koong A, Kaper F, Chen E, Gottschalk AR, Ryan HE, Johnson RS, Jefferson AB, Stokoe D and Giaccia AJ: Loss of PTEN facilitates HIF-1-mediated gene expression. Genes Dev 14: 391-396, 2000.

J Periodont Res 2007; 42: 283 286

JOURNAL OF PERIODONTAL RESEARCH
doi:10.1111/j.1600-0765.2006.00944.x

Identification of marker genes distinguishing human periodontal ligament cells from human mesenchymal stem cells and human gingival fibroblasts

T. Fujita[1], T. Iwata[1], H. Shiba[1], A. Igarashi[3], R. Hirata[1], K. Takeda[1], N. Mizuno[1], K. Tsuji[3], H. Kawaguchi[1], Y. Kato[2,3], H. Kurihara[1]

[1]Department of Periodontal Medicine, Division of Frontier Medical Science and [2]Department of Dental and Medical Biochemistry, Division of Molecular Medical Science, Hiroshima University Graduate School of Biomedical Science, Hiroshima, Japan and [3]Two cells Co. Ltd, Hiroshima, Japan

Fujita T, Iwata T, Shiba H, Igarashi A, Hirata R, Takeda K, Mizuno N, Tsuji K, Kawaguchi H, Kato Y, Kurihara H. Identification of marker genes distinguishing human periodontal ligament cells from human mesenchymal stem cells and human gingival fibroblasts. J Periodont Res 2007; 42: 283–286. © 2006 The Authors. Journal compilation © 2006 Blackwell Munksgaard

Background and Objective: Molecular gene markers, which can distinguish human bone marrow mesenchymal stem cells from human fibroblasts, have recently been reported. Messenger RNA levels of tissue factor pathway inhibitor-2, major histocompatibility complex-DR-α, major histocompatibility complex-DR-β, and neuroserpin are higher in human bone marrow mesenchymal stem cells than in human fibroblasts. However, human bone marrow mesenchymal stem cells express less apolipoprotein D mRNA than human fibroblasts. Periodontal ligament cells are a heterogeneous cell population including fibroblasts, mesenchymal stem cells, and progenitor cells of osteoblasts or cementoblasts. The use of molecular markers that distinguish human bone marrow mesenchymal stem cells from human fibroblasts may provide insight into the characteristics of human periodontal ligament cells. In this study, we compared the molecular markers of human periodontal ligament cells with those of human bone marrow mesenchymal stem cells and human gingival fibroblasts.

Material and Methods: The mRNA expression of the molecular gene markers was analyzed using real-time polymerase chain reaction. Statistical differences were determined with the two-sided Mann–Whitney *U*-test.

Results: Messenger RNA levels of major histocompatibility complex-DR-α and major histocompatibility complex-DR-β were lower and higher, respectively, in human periodontal ligament cells than in human bone marrow mesenchymal stem cells or human gingival fibroblasts. Human periodontal ligament cells showed the lowest apolipoprotein D mRNA levels among the three types of cells.

Conclusion: Human periodontal ligament cells may be distinguished from human bone marrow mesenchymal stem cells and human gingival fibroblasts by the genes for apolipoprotein D, major histocompatibility complex-DR-α, and major histocompatibility complex-DR-β.

Tsuyoshi Fujita, Department of Periodontal Medicine, Division of Frontier Medical Science, Hiroshima University Graduate School of Biomedical Science, 1-2-3, Kasumi, Minami-ku, Hiroshima 734–8553, Japan
Tel: +81 82 2575663
Fax: +81 82 2575664
e-mail: tfuji@hiroshima-u.ac.jp

Key words: apolipoprotein D; human periodontal ligament cells; molecular gene marker

Accepted for publication August 3, 2006

Bone marrow mesenchymal stem cells, also called plastic-adherent marrow cells or bone marrow stromal cells, can differentiate into osteoblasts, chondrocytes, adipocytes, tenocytes, and muscle cells *in vitro and in vivo* (1–3). A recent study has identified several molecular marker genes that distinguish human bone marrow mesenchymal stem cells from human fibroblasts (4). The mRNA levels of major histocompatibility complex-DR-α, major histocompatibility complex-DR-β, tissue factor pathway inhibitor-2, and neuroserpin were all higher in human bone marrow mesenchymal stem cells than in fibroblasts. On the other hand, the mRNA levels of adrenomedullin, apolipoprotein D, C-type lectin superfamily member-2, collagen type XV α1, CUG triplet repeat RNA-binding protein, matrix metalloproteinase (MMP)-1, protein tyrosine kinase-7 and Sam68-like phosphotyrosine protein/T-STAR levels were lower in human bone marrow mesenchymal stem cells than in fibroblasts. Thus, the identified marker genes may be useful for regenerative medicine with bone marrow mesenchymal stem cells (4).

The periodontal ligament is a connective tissue between two mineralized tissues – alveolar bone and cementum. Periodontal ligament cells are a heterogeneous cell population, containing fibroblasts and progenitor cells, which can differentiate into osteoblasts and cementoblasts, and have osteoblast-like properties, such as high levels of alkaline phophatase activity and production of bone-associated proteins (5–9). The gene expression pattern of periodontal ligament cells is different from that of gingival fibroblasts (10–12). Periodontal ligament tissue has recently been found to contain mesenchymal stem cells, in addition to osteoprogenitor cells and fibroblasts (13–16). The identification of molecular markers, which distinguish periodontal ligament cells from bone marrow mesenchymal stem cells, as well as from gingival fibroblasts, may aid in the characterization of periodontal ligament cells.

In the present study, we compared the characteristics of human periodontal ligament cells with those of human bone marrow mesenchymal stem cells and human gingival fibroblasts by examining the expression of molecular gene markers distinguishing human bone marrow mesenchymal stem cells from human fibroblasts.

Material and methods

Preparation of human periodontal ligament cells and human gingival fibroblasts

Human periodontal ligament cells-1, -2, -3, and -4 were obtained separately by the explant culture of healthy periodontal ligament from the mid-root of four premolars extracted (after obtaining informed consent) from four patients undergoing orthodontic treatment. Human gingival fibroblasts were obtained separately from four healthy gingival tissue explants from four different volunteers. Informed consent was obtained under a protocol approved by the Ethics Committee of the Hiroshima University (Hiroshima, Japan) Faculty of Dentistry. Periodontal ligament tissue and human gingival tissue were cut into small pieces and plated in 35-mm culture dishes (Corning Inc., Corning, NY, USA) containing Dulbecco's modified Eagle's medium (Sigma, St Louis, MO, USA) supplemented with 10% fetal bovine serum (Hyclone, South Logan, UT, USA), 100 units/ml of penicillin, 100 μg/ml of streptomycin, and 1 μg/ml of amphotericin B (Medium A). When the human periodontal ligament cells or the human gingival fibroblasts formed a confluent monolayer, they were harvested and seeded on a 100-mm culture dish (Corning) in the presence of medium A. Human periodontal ligament cells at the sixth passage, or human gingival fibroblasts at the fourth passage, were used in the experiments.

Preparation of human bone marrow mesenchymal stem cells

Human bone marrow mesenchymal stem cells-1, -2, -3, and -4 were obtained from the iliac crest of four patients. Informed consent was obtained under a protocol approved by the Ethics Committee of the Hiroshima University Faculty of Dentistry. Bone marrow cells, including erythrocytes, were seeded at a density of 0.1 ml of aspirate per 35-mm tissue culture dish and maintained in 2 ml of medium A. Three days after the seeding, floating cells were removed and the medium was replaced with fresh medium A. Thereafter, attached cells were fed with fresh medium A supplemented with 1 ng/ml of fibroblast growth factor-2 (Kaken Pharmaceutical Co., Ltd. Tokyo, Japan). Fibroblast growth factor-2 was added every other day (17). Passages were performed when the cells became subconfluent. Human bone marrow mesenchymal stem cells at the fourth passage were used for the experiments.

RNA preparation

Human periodontal ligament cells-1, -2, -3, and -4 at the sixth passage, human gingival fibroblasts-1, -2, -3, and -4 at the fourth passage, or human bone marrow mesenchymal stem cells-1, -2, -3, and -4 at the fourth passage were harvested, seeded at a density of 7×10^4 cells per 60-mm culture dish coated with type I collagen, and maintained in 5 ml of medium A. After 10 d of culture, the confluent cells were washed three times with phenol red-free Hank's solution (pH 7.4). Total RNA was extracted from each cell using ISOGEN® (Wako Pure Chemical Industries, Osaka, Japan) and quantified by spectrometry at 260 and 280 nm.

Real time polymerase chain reaction

First-strand DNAs were synthesized with 1 μg of total RNA using the SuperScript first-strand synthesis system (Invitrogen, Carlsbad, CA, USA). Real-time polymerase chain reaction (PCR) with the cDNAs was performed using an ABI 7900 system (Applied Biosystems, Tokyo, Japan). The TaqMan probe, sense primers, and antisense primers used for detection are listed in Table 1. A commercially available human glyceraldehyde-3-phosphate dehydrogenase (Applied Biosystems) was used for quantitative PCR.

Table 1. Primers and probes for real-time polymerase chain reaction

Gene name	Primer	
TFPI-2	Forward	5′-GGCAACGCCAACAATTTCTAC-3′
	Reverse	5′-CAAACTTTGGGAACTTTTTCTATCCT-3′
	Probes	5′-CTGGGAGGCTTGCGACGATGC-3′
Neuroserpin	Forward	5′-TGGGTGGAGAATAACACAAACAA-3′
	Reverse	5′-CCAGATAAGTGGCAGCATCAAA-3′
	Probes	5′-CTGGTGAAAGATTTGGTATCCCCAAGGG-3′
MHC-DR-α	Forward	5′-GCCCAGGGAAGACCACCTT-3′
	Reverse	5′-CAGTCGTAAACGTCCTCAGTTGA-3′
	Probes	5′-TCCGCAAGTTCCACTATCTCCCCTTCCT-3′
MHC-DR-β	Forward	5′-GGCTGAAGTCCAGAGTGTCCTT-3′
	Reverse	5′-GCTGGGCCTGCTCTTCCT-3′
	Probes	5′-CCTGAAGTAGATGAACAGCCCGGCC-3′
Apolipoprotein D	Forward	5′-TGAGAAGATCCCAACAACCTTTG-3′
	Reverse	5′-TGATCTTTCCGTTTTCCATTAGTG-3′
	Probes	5′-ATGGACGCTGCATCCAGGCCAACTA-3′
Adrenomedullin	Forward	5′-GGTTTCCGTCGCCCTGAT-3′
	Reverse	5′-GAGCCCACTTATTCCACTTCTTTC-3′
	Probes	5′-ACCTGGGTTCGCTCGCCTTCCTAG-3′
CUG triplet repeat	Forward	5′-CATGAATGCTTTACAGTTGCAGAA-3′
RNA-binding protein 2	Reverse	5′-GCGCTGCTCGTGGTAGAGA-3′
	Probes	5′-CTCAGCCACCAGCACCAATGCAAAC-3′
C-type lectin	Forward	5′-ATCCATTTTCTTTCGGTGTAACATCTA-3′
	Reverse	5′-CATGAGAGGGAGTGAAGGATGTG-3′
	Probes	5′-CTGTTGCTGCACCATCATCGCTGAG-3′
Collagen type XV α1	Forward	5′-CCAGCAACCCACATCAGCTT-3′
	Reverse	5′-ATGCAGAGCAGGCTTCTCATAAT-3′
	Probes	5′-TGCCTCCACCAAACCCTATTTCAAGTGC-3′
MMP-1	Forward	5′-GATGGACCTGGAGGAAATCTTG-3′
	Reverse	5′-CCGCAACACGATGTAAGTTGTACT-3′
	Probes	5′-TCATGCTTTTCAACCAGGCCCAGGTATT-3′

MMP, matrix metalloproteinase; MHC-DR-α, major histocompatibility complex-DR-α; MHC-DR-β, major histocompatibility complex-DR-β; TFPI-2, tissue factor pathway inhibitor.

Statistical analysis

The statistical differences between human periodontal ligament cells and human bone marrow mesenchymal stem cells, and between human periodontal ligament cells and human gingival fibroblasts, were determined with the two-sided Mann- Whitney *U*-test. Differences with a p-value of < 0.05 were considered significant.

Results

Messenger RNA levels of apolipoprotein D were lower in human periodontal ligament cells than in either human bone marrow mesenchymal stem cells or human gingival fibroblasts (Table 2). Human periodontal ligament cells also had lower levels of neuroserpin than human bone marrow mesenchymal stem cells, but not human gingival fibroblasts (Table 2). Messenger RNA levels of major histocompatibility complex-DR-α and major histocompatibility complex-DR-β were lower and higher, respectively, in human periodontal ligament cells than in human bone marrow mesenchymal stem cells or human gingival fibroblasts (Table 2). Human periodontal ligament cells had higher levels of tissue factor pathway inhibitor-2 mRNA than did human gingival fibroblasts but not human bone marrow mesenchymal stem cells (Table 2). No significant differences between human periodontal ligament cells and human bone marrow mesenchymal stem cells, or between human periodontal ligament cells and human gingival fibroblasts, were observed in the mRNA levels of Type XV collagen and adenomedullin (Table 2). On the other hand, CUG triplet repeat RNA-binding protein, C-type lectin, and MMP-1 mRNA levels were lower in human periodontal ligament cells than in human gingival fibroblasts, although no significant difference was found between human periodontal ligament cells and human bone marrow mesenchymal stem cells in the expression of these mRNAs (Table 2). The findings, regarding the expression of these 10 genes in human bone marrow mesenchymal stem cells compared with human gingival fibroblasts, are consistent with those of a previous report (4).

Discussion

Because human periodontal ligament cells, human bone marrow mesenchymal stem cells, and human gingival fibroblasts are spindle-like cells, human periodontal ligament cells have not been characterized by their morphology. For the first time, the present study demonstrated that the genes for apolipoprotein D, major histocompatibility complex-DR-α, and major histocompatibility complex-DR-β are candidates for molecular markers distinguishing human periodontal ligament cells from human bone marrow mesenchymal stem cells and human gingival fibroblasts.

In the present study, the mRNA expressions of major histocompatibility complex-DR-α and -β, and tissue factor pathway inhibitor-2 were lower in human gingival fibroblasts than in human periodontal ligament cells. On the other hand, the mRNA expressions of apolipoprotein D, CUG triplet repeat RNA-binding protein, C-type lectin, and MMP-1 were higher in human gingival fibroblasts than in human periodontal ligament cells. Regarding MMP-1 expression, the present finding is consistent with the previous report on DNA array analysis (10).

Apolipoprotein D is known to participate in maintenance and repair within the central and peripheral nervous systems (18). The present study found that human gingival fibroblasts show the highest mRNA levels of apolipoprotein D among human gingival fibroblasts, human bone marrow mesenchymal stem cells, and human periodontal ligament cells. Human bone marrow mesenchymal stem cells can differentiate into neurons (19). However, to our knowledge, there is no report regarding the involvement of

Table 2. Comparison of gene expressions between human periodontal ligament (HPL) cells and human bone marrow mesenchymal stem cells (hMSC) and between HPL cells and human gingival fibroblasts (HGF)

	Cells							
	HPL cells		hMSC			HGF		
Genes	-1 -3	-2 -4	-1 -3	-2 -4		-1 -3	-2 -4	
Apolipoprotein D	0.44	0.63	1.21	1.03	*	81.31	7.83	**
	0.11	0.03	1.19	0.54		159.9	175.6	
Neuroserpin	0.31	0.72	0.78	1.21	*	0.16	0.56	
	0.16	0.32	1.33	0.66		0.18	0.45	
MHC-DR-α	0.12	0.03	0.95	0.48	*	0.01	0.03	**
	0.18	0.14	1.55	10.64		0.001	0.001	
MHC-DR-β	0.18	0.01	1.34	0.65	*	0.01	0.01	**
	0.27	0.08	6.89	63.25		0.001	0.001	
TFPI-2	0.50	0.70	1.52	0.29		0.03	0.09	**
	0.19	0.31	1.30	0.87		0.11	0.12	
Adrenomodullin	0.45	1.34	0.66	1.49		0.38	1.96	
	0.31	0.23	1.13	0.69		10.79	14.38	
CUG triplet repeat	0.09	0.39	0.19	1.52		4.53	0.73	**
RNA-binding protein 2	0.52	0.91	1.06	0.40		11.88	18.41	
C-type lectin	6.06	0.42	0.52	0.81		13.59	11.69	**
	1.79	0.55	1.65	0.01		9.30	18.77	
Collagen type XV α1	0.63	11.06	0.19	1.95		2.43	4.62	
	3.43	0.07	6.28	0.85		74.15	81.31	
MMP-1	14.7	22.32	16.99	0.76		4218	1306	**
	2.97	10.29	5.96	1.23		99.57	80.75	

Values are arbitrary ratios of each mRNA to glyceraldehyde-3-phosphate dehydrogenase mRNA.
*Significantly different between human periodontal ligament cells and hMSC; $p < 0.05$.
**Significantly different between human periodontal ligament cells and human gingival fibroblasts; $p < 0.05$.
MMP, matrix metalloproteinase; MHC-DR-α, major histocompatibility complex-DR-α; MHC-DR-β, major histocompatibility complex-DR-β; TFPI-2, tissue factor pathway inhibitor.

fibroblasts in the functioning of neurons. Therefore, the higher levels of expression suggest a new role for apolipoprotein D in the functioning of gingival fibroblasts.

Tissue factor pathway inhibitor-2 is thought to play an important role in the regulation of extracellular matrix in digestion and remodeling (20,21). Periodontal ligament tissue is thought to be more actively remodeled than gingival tissue. The active remodeling of periodontal ligament tissue may be a result of increased levels of tissue factor pathway inhibitor-2.

In conclusion, the genes for apolipoprotein D, major histocompatibility complex-DR-α, and major histocompatibility complex-DR-β are suggested to be molecular markers characterizing periodontal ligament cells. The role of the markers in periodontal ligament needs to be studied further.

References

1. Pittenger MF, Mackay AM, Beck SC *et al.* Multilineage potential of adult human mesenchymal stem cells. *Science* 1999;284:143–147.
2. Pereira RF, Halford KW, O'Hara MD *et al.* Cultured adherent cells from marrow can serve as long-lasting precursor cells for bone, cartilage, and lung in irradiated mice. *Proc Natl Acad Sci USA* 1995;92:4857–4861.
3. Jiang Y, Jahagirdar BN, Reinhardt RL *et al.* Pluripotency of mesenchymal stem cells derived from adult marrow. *Nature* 2002;418:41–49.
4. Ishii M, Koike C, Igarashi A *et al.* Molecular markers distinguish bone marrow mesenchymal stem cells from fibroblasts. *Biochem Biophys Res Commun* 2005;332:297–303.
5. Gould TR, Melcher AH, Brunette DM. Location of progenitor cells in periodontal ligament of mouse molar stimulated by wounding. *Anat Rec* 1977;188:133–141.
6. McCulloch CA. Progenitor cell populations in the periodontal ligament of mice. *Anat Rec* 1985;211:258–262.
7. Nanci A, Bosshardt DD. Structure of periodontal tissues in health and disease. *Periodontol 2000* 2006;40:11–28.
8. Matsuura M, Herr Y, Han KY, Lin WL, Genco RJ, Cho MI. Immunohistochemical expression of extracellular matrix components of normal and healing periodontal tissues in the beagle dog. *J Periodontol* 1995;66:579–593.
9. Nohutcu RM, McCauley LK, Koh AJ, Somerman MJ. Expression of extracellular matrix proteins in human periodontal ligament cells during mineralization *in vitro*. *J Periodontol* 1997;68:320–327.
10. Han X, Amar S. Identification of genes differentially expressed in cultured human periodontal ligament fibroblasts vs. human gingival fibroblasts by DNA microarray analysis. *J Dent Res* 2002;81:399–405.
11. Park JC, Kim YB, Kim HJ *et al.* Isolation and characterization of cultured human periodontal ligament fibroblast-specific cDNAs. *Biochem Biophys Res Commun* 2001;282:1145–1153.
12. Yamamoto T, Myokai F, Nishimura F *et al.* Gene profiling in human periodontal ligament fibroblasts by subtractive hybridization. *J Dent Res* 2003;82:641–645.
13. Morsczeck C, Gotz W, Schierholz J *et al.* Isolation of precursor cells (PCs) from human dental follicle of wisdom teeth. *Matrix Biol* 2005;24:155–165.
14. Miura M, Gronthos S, Zhao M *et al.* SHED. stem cells from human exfoliated deciduous teeth. *Proc Natl Acad Sci USA* 2003;100:5807–5812.
15. Gronthos S, Mankani M, Brahim J, Robey PG, Shi S. Postnatal human dental pulp stem cells (DPSCs) *in vitro* and *in vivo*. *Proc Natl Acad Sci USA* 2000; 97:13625–13630.
16. Seo BM, Miura M, Gronthos S *et al.* Investigation of multipotent postnatal stem cells from human periodontal ligament. *Lancet* 2004;364:149–155.
17. Tsutsumi S, Shimazu A, Miyazaki K *et al.* Retention of multilineage differentiation potential of mesenchymal cells during proliferation in response to FGF. *Biochem Biophys Res Commun* 2001;288:413–419.
18. Rassart E, Bedirian A, Do Carmo S *et al.* Apolipoprotein D. *Biochim Biophys Acta* 2000;1482:185–198.
19. Krabbe C, Zimmer J, Meyer M. Neural transdifferentiation of mesenchymal stem cells – a critical review. *Apmis* 2005; 113:831–844.
20. Lwaleed BA, Bass PS. Tissue factor pathway inhibitor: structure, biology and involvement in disease. *J Pathol* 2006; 208:327–339.
21. Chand HS, Foster DC, Kisiel W. Structure, function and biology of tissue factor pathway inhibitor-2. *Thromb Haemost* 2005;94:1122–1130.

Multiple Mechanisms Regulate Circadian Expression of the Gene for Cholesterol 7α-Hydroxylase (*Cyp7a*), a Key Enzyme in Hepatic Bile Acid Biosynthesis

Mitsuhide Noshiro,*[,1] Emiko Usui,* Takeshi Kawamoto,* Hiroshi Kubo,* Katsumi Fujimoto,* Masae Furukawa,† Sato Honma,‡ Makoto Makishima,§ Ken-ichi Honma,‡ and Yukio Kato*

*Department of Dental and Medical Biochemistry, †Department of Prosthetic Dentistry, Hiroshima University Graduate School of Biomedical Sciences, Hiroshima, ‡Department of Physiology, Hokkaido University Graduate School of Medicine, Sapporo, §Department of Biochemistry, Nihon University School of Medicine, Tokyo, Japan

Abstract Cholesterol 7α-hydroxylase (CYP7A) and sterol 12α-hydroxylase (CYP8B) in bile acid biosynthesis and 3-hydroxyl-3-methylglutaryl CoA reductase (HMGCR) in cholesterol biosynthesis are the key enzymes in hepatic metabolic pathways, and their transcripts exhibit circadian expression profiles in rodent liver. The authors determined transcript levels of these enzymes and the regulatory factors for *Cyp7a*—including *Dbp*, *Dec2*, *E4bp4*, *Hnf4α*, *Pparα*, *Lxrα*, *Rev-erbα*, and *Rev-erbβ*—in the liver of wild-type and homozygous *Clock* mutant mice (*Clock/Clock*) and examined the effects of these transcription factors on the transcription activities of *Cyp7a*. The expression profile of the *Cyp7a* transcript in wild-type mice showed a strong circadian rhythm in both the 12L:12D light-dark cycle and constant darkness, and that in *Clock/Clock* also exhibited a circadian rhythm at an enhanced level with a lower amplitude, although its protein level became arrhythmic at a high level. The expression profile of *Cyp8b* mRNA in wild-type mice showed a shifted circadian rhythm from that of *Cyp7a*, becoming arrhythmic in *Clock/Clock* at an expression level comparable to that of wild-type mice. The expression profile of *Hmgcr* mRNA also lost its strong circadian rhythm in *Clock/Clock*, showing an expression level comparable to that of wild-type mice. The expressions of *Dbp*, *Dec2*, *Rev-erbα*, and *Rev-erbβ*—potent regulators for *Cyp7a* expression—were abolished or became arrhythmic in *Clock/Clock*, while other regulators for *Cyp7a*—*Lxrα*, *Hnf4α*, *Pparα*, and *E4bp4*—had either less affected or enhanced expression in *Clock/Clock*. In luciferase reporter assays, REV-ERBα/β, DBP, LXRα, and HNF4α increased the promoter activity of *Cyp7a*, whereas DEC2 abolished the transcription from the *Cyp7a* promoter: E4BP4 and PPARα were moderate negative regulators. Furthermore, knockdown of REV-ERBα/β with siRNA suppressed *Cyp7a* transcript levels, and in the electrophoretic mobility shift assay, REV-ERBα/β bound to the promoter of *Cyp7a*. These observations suggest that (1) active CLOCK is essential for the robust circadian expression of hepatic metabolic enzymes (*Cyp7a*, *Cyp8b*, and *Hmgcr*); (2) clock-controlled genes—DBP, DEC2, and REV-ERBα/β—are direct regulators required for the robust circadian rhythm of *Cyp7a*; and (3) the circadian rhythm of *Cyp7a* is regulated by multiple transcription factors, including DBP, REV-ERBα/β, LXRα, HNF4α DEC2, E4BP4, and PPARα.

Key words CLOCK, CYP7A, CYP8B, HMGCR, DEC2, DBP, REV-ERB, LXRα

JOURNAL OF BIOLOGICAL RHYTHMS, Vol. 22 No. 4, August 2007 299-311
DOI: 10.1177/0748730407302461

A mammalian master clock located in the SCN of the hypothalamus drives circadian rhythms in behavior and physiology and entrains to the environmental light cycle. Rhythms in the SCN are thought to stem from interlocked transcription-translation feedback loops composed of the positive elements CLOCK and BMAL1, as well as negative elements PERIODs (PER1, PER2, and PER3), CRYPTOCHROMEs (CRY1 and CRY2), and DECs (DEC1 and DEC2) (Reppert and Weaver, 2001; Honma et al., 2002; Kawamoto et al., 2004). CLOCK and BMAL1 dimerize and act on CACGTG E-boxes to promote transcription of *Per*, *Cry*, *Dec*, and other genes, and translated PERs, CRYs, and DECs associate and inhibit CLOCK:BMAL1 transactivation of the *Per*, *Cry*, and *Dec* genes (Alvarez and Sehgal, 2002). In addition, the high binding affinity of DECs to the CACGTG E-box and similar elements is another potent mechanism suppressing the transactivation of target genes by CLOCK:BMAL1 (Hamaguchi et al., 2004; Kawamoto et al., 2004). Other feedback loops control the positive clock element: Orphan nuclear receptors—ROR(α, β, and γ) and REV-ERB (α and β)—activate and repress *Bmal1* transcription, respectively, by competing with the REV-ERB/ROR response element (RRE) (Nakajima et al., 2004; Sato et al., 2004; Guillaumond et al., 2005). Thus, multiple feedback loops are interlocked, which may be essential for the finer and more stabilized regulation of circadian rhythm (Roenneberg and Merrow, 2003; Kawamoto et al., 2004). DECs as well as other clock-related genes regulate numerous target genes in output pathways.

Recently, the existence of peripheral clocks has been clarified in most peripheral organs, including the liver, kidney, and heart: These clocks apparently serve as endogenous oscillators in the regulation of the peripheral circadian rhythms and are synchronized with the master clock in expressing orchestrated circadian rhythms in peripheral tissues (Sakamoto et al., 1998; Panda et al., 2002; Storch et al., 2002). The liver is the crucial organ for energy metabolism, detoxification, and nutrient absorption—such as biosynthesis and secretion of bile acids—and more than 300 circadian rhythms have recently been detected in hepatic transcripts (Panda et al., 2002; Ueda et al., 2002), which encode the proteins involved in these functions. Actually, up to 20% of soluble proteins are subject to circadian control and play important roles in hepatic metabolic pathways (Reddy et al., 2006). Cholesterol 7α-hydroxylase (CYP7A) is a rate-limiting enzyme for bile acid production, and it is expressed in a circadian-dependent fashion (Noshiro et al., 1990; Russell, 1992; Ishida et al., 2000). Numerous transcription factors are known to regulate the expression of *Cyp7a*. DBP, a PAR (proline and acidic amino acid rich) basic leucine zipper transcription factor, amplifies the circadian *Cyp7a* rhythm, and multiple DBP-responsive elements (D-box) in the 5′-upstream of *Cyp7a* have been identified (Lavery and Schibler, 1993; Lee et al., 1994). In addition, several nuclear receptors—including LXRα, HNF4α, PPARα, and RXRα—are involved in the regulation of *Cyp7a* (Chiang, 2002). Furthermore, our recent work demonstrated that the *Cyp7a* transcription enhanced by DBP was strongly suppressed by DEC2 and E4BP4, which bind the proximal E-box (CACATG) and D-box, respectively, even though CACATG E-box is not responsive to the CLOCK:BMAL1 heterodimer (Noshiro et al., 2004).

The *Clock* mutant mouse (*Clock/Clock*) is a useful animal model for examining potential up-regulation of genes by CLOCK. Mutant CLOCK protein with a 51-amino acid deletion acts in a dominant-negative fashion (King et al., 1997; Gekakis et al., 1998): The expression profiles of many clock genes, such as *Pers*, *Crys*, and *Decs*, are disrupted with reduced peak expression in the SCN of *Clock/Clock* mice (Jin et al., 1999; Kume et al., 1999; Oishi et al., 2000; Butler et al., 2004). Attenuation of clock gene expressions in *Clock/Clock* mice indicates that CLOCK activates these genes in vivo.

We wanted to determine whether a regulatory cascade induces a hepatic oscillating target gene, *Cyp7a*, from the peripheral clock consisting of clock genes: We tested the effects of *Clock* mutation on the circadian expression of *Cyp7a* in the liver by examining transcript levels of *Cyp7a*, along with other hepatic oscillating enzymes—*Cyp8b* and *Hmgcr*—and several known and possible regulatory factors for *Cyp7a* in the liver of wild-type mice and *Clock/Clock* mice. We also examined the effects of those transcription factors on the transcription activities of the *Cyp7a* gene using luciferase reporter assays: In the liver of *Clock/Clock* mice, the expressions of *Dbp*, *Dec2*, and *Rev-erbα* were abolished and became arrhythmic, and in luciferase reporter assays, these factors were potent regulators for

1. To whom all correspondence should be addressed: Mitsuhide Noshiro, Department of Dental and Medical Biochemistry, Hiroshima University Graduate School of Biomedical Sciences, Kasumi 1-2-3, Hiroshima 734-8553, Japan; e-mail: noshiro@hiroshima-u.ac.jp.

the transcription from the *Cyp7a* promoter. Even so, the *Cyp7a* expression profile in the liver of *Clock/Clock* mice exhibited a circadian rhythm at an enhanced level with lower amplitude. Expressions of other known positive and negative regulators for *Cyp7a*—*Lxrα*, *Hnf4α*, *E4bp4*, and *Pparα*—were enhanced or remained unchanged in *Clock/Clock* mice, and those regulators may support both the enhanced *Cyp7a* expression and the rhythmicity. These observations strongly indicate that multiple regulators support the circadian regulation of *Cyp7a*.

MATERIALS AND METHODS

Animals and Isolation of RNA

A breeding colony of *Clock* mutant mice with a BALB/c background was developed using mice originally supplied by Dr. J. S. Takahashi (Northwestern University) as described previously (Nakamura et al., 2002). Both *Clock* mutant and wild-type mice were housed in clear polycarbonate cages in a 12h:12h light-dark cycle (lights on at 0600 h) with ad libitum access to food and water. All procedures were performed in compliance with principles and guidelines for animal research established by the following local care and use committee: Guide for the Care and Use of Laboratory Animals, Hokkaido University Graduate School of Medicine.

Mice were decapitated at 4-h intervals beginning at ZT2 (0800 h) either in a normal LD cycle or on the first day of constant darkness (DD)—that is, beginning 14 h after the last lights-off. A dim red light (< 0.1 lux) was placed in the room during the dark phase to allow surgery during the dark periods. Extraction of total RNA from mouse liver was described previously (Noshiro et al., 2005).

Real-Time Quantitative RT-PCR Analysis

Real-time quantitative reverse-transcription PCR (RT-PCR) analysis was performed using an ABI PRISM 7900 Sequence Detection System instrument and software (Applied Biosystems, Foster City, CA) as described previously (Gibson et al., 1996). First-strand cDNA was synthesized using a ReverTra Ace reverse transcriptase kit (Toyobo Co., Osaka, Japan) with total RNA (1 μg) preparations and random primers. Validity of the cDNA preparations was examined by amplification of 18S ribosomal RNA using the Ribosomal RNA control kit (Applied Biosystems). The sequences for the primers and TaqMan™ fluorogenic probes (Applied Biosystems) were as follows: 5′-ACTCTCTGAAGCCATGATGCAAA-3′, 5′-TCCCAGACAGCGCTCTTTGAT-3′, and 5′-FAM-TGCAAAACCTCCAATCTGTCATGAGACCTC-TAMRA-3′ for Cyp7a (L23754); 5′-GGCTGGCTTCCTGAGCTTATT-3′, 5′-ACTTCCTGAACAGCTCATCGG-3′, and 5′-FAM-CAAGGACAAGCAGCAAGACCTGGATGAG-TAMRA-3′ for Cyp8b (AF090317); 5′-CTTGGTCCTTGTTCACGCTCA-3′, 5′-ACCTTAGCCTGCTCCGCTGTGCTG-3′, and 5′-FAM-AGTCGCTGGATAGCTGATCCTTCTCCTCA-TAMRA-3′ for Hmgcr (BC019782); 5′-CATTCAAGATTGGTCCCTCA-3′, 5′-GAAGCTACTCTGAGTTTTGC-3′, and 5′-FAM-ATCGGAACACTGGCATCACAAAGAACTG-TAMRA-3′ for E4bp4 (U83148); 5′-TTCCCACGGATGCTAATGAAG-3′, 5′-GGAAGCTTTTTGTCCTGCAGG-3′, and 5′-FAM-ACTTTGAGCAGCGTCCATTCAGAGCAAGT-TAMRA-3′ for α (NM_013839); 5′-GGTCCATGGTGTTTAAGGACGT-3′, 5′-ACGGCTCATCTCCGCTAGCTCT-3′, and 5′-FAM-CAATGACTACATCGTCCCTCGGCACTGT-TAMRA-3′ for HNF4α (XM_110385); and 5′-CCTCCTTGATGAACAAAGACGG-3′, 5′-TTCTTAAGGAACTCGCGTGTGA-3′, and 5′-FAM-CTGATCGCGTACGGCAATGGCTT-TAMRA-3′ for PPARα (NM_011144). Those for *Dbp*, *Dec2*, and *Rev-erbα* were previously described (Noshiro et al., 2005). The primers and TaqMan™ probe for *Rev-erbβ* were obtained from Applied Biosystems.

Western Blot Analysis

Microsomal fractions were prepared from liver homogenates by centrifugation as described previously (Noshiro and Omura, 1978). Nuclear extracts were also prepared from the livers by the use of the Nuclear Extract Kit (Active Motif, Carlsbad, CA). After sodium dodecyl sulfate–polyacrylamide gel electrophoresis (SDS-PAGE), proteins were transferred to polyvinylidene difluoride membrane (Millipore, Bedford, MA). Immunoblotting was performed with the appropriate antibodies according to standard protocols and detected using ^{125}I-labeled antimouse antibodies or ^{125}I-labeled antirabbit antibodies (GE Healthcare Bioscience, Uppsala, Sweden) as second antibodies. The following primary antibodies were used: mouse polyclonal antibodies to CYP7A (1:1000 dilution) (Noshiro et al., 1990) and rabbit polyclonal antibodies to LXRα (1:1000 dilution, Santa Cruz Biotechnology Inc., Santa Cruz, CA). Radioactivity of detected areas was quantified using

the FLA-3000C fluoro-image analyzer (Fuji Photo Film Co. Ltd., Tokyo, Japan).

Luciferase Assay

Experimental conditions for human HepG2 cell culture, DNA transfection to the cells, and assay of luciferase activity were described previously (Noshiro et al., 2004). A DNA fragment containing 766 bp (-731 to +35) of rat *CYP7A* gene promoter was used to construct pCYP7A-Luc as described (Noshiro et al., 2004). The expression plasmids (pcDNA3.1) for mouse DBP and DEC2 were prepared as described previously (Noshiro et al., 2004). The expression plasmids (pCMX) for mouse PPARα (NR1C1), rat HNF4α (NR2A1), rat E4BP4, mouse LRH-1 (NR5A2), human LXRα (NR1H3), and human RXRα (NR2B1) were described previously (Kliewer et al., 1994; Willy et al., 1995; Lu et al., 2000). The expression plasmid for mouse REV-ERBα (NR1D1) was obtained by RT-PCR with primers 5′-CGCCACCATGACGACCCTGGACTCCAATA-3′ and 5′-GGAGAGAGAAGTGCAGAGTT-3′ and cloning into pcDNA3.1 (Invitrogen, Carlsbad, CA). The expression plasmids for other orphan nuclear receptors, REV-ERBβ (NR1D2), RORα (NR1F1), and RORβ (NR1F2), were generous gifts from Dr. Masaaki Ikeda (Saitama Medical School).

Short Interfering RNA (siRNA) Treatment

The siRNAs to be directed against *Rev-erbα* and *Rev-erbβ* were prepared. The target sequences were 5′-CUAUGCCCAUGACAAGUUAGG-3′ and GGAGGAACAUAAUGCAUUACC-3′ for *Rev-erbα* and *Rev-erbβ*, respectively. Mouse hepatoma Hepa-1c1c7 cells (American Type Culture Collection, Manassas, VA) were plated at a density 7.5×10^4 cells/well in 12-multiwell plastic plates. The next day, the cells were transfected with the siRNA or nonspecific control siRNA (Qiagen, Valencia, CA) at a final concentration of 25 nM using Lipofectamine 2000 (Invitrogen). Efficiency of transfection was nearly 100% as assessed with a fluorescein-labeled RNA probe (data not shown). The cells were harvested at 72 h after transfection and subjected to RNA preparation.

Electrophoretic Mobility Shift Assay

Double-stranded synthetic probes for the electrophoretic mobility shift assay (EMSA) were prepared and labeled with α-[^{32}P]dCTP as described previously (Noshiro et al., 2004). The binding reaction mixture contained 20,000 cpm of labeled oligonucleotide probe and the protein factor(s) in 15 μL of 10 mM Tris-HCl (pH 8.0), 50 mM NaCl, 25 mM $MgCl_2$, 5 mM dithiothreitol, 0.2 μg/μL poly (dI-dC), and 10% glycerol. The mixtures were incubated at room temperature for 10 min and subjected to 5% acrylamide gel electrophoresis. Electrophoresis was performed at room temperature for 1.5 h at constant 15W. The protein factors were prepared by the use of TnT Quick coupled in vitro transcription/translation system (Promega, Madison, WI) and the expression plasmids.

Statistical Analysis

Time-series data were examined by 1-way analysis of variance (ANOVA) for rhythmicity, and differences between genotypes were tested by 2-way ANOVA. Significance of differences between the 2 groups was analyzed by Student *t* test. Comparisons with $p < 0.05$ were taken as significant.

RESULTS

Effects of *Clock* Mutation on the Circadian Expression of *Cyp7a*, *Cyp8b*, and *Hmgcr*

First, to determine whether *Clock* mutation affected *Cyp7a* expression, its transcript levels in the livers of 2 genotypes were determined. Quantitative real-time RT-PCR analysis showed that *Cyp7a* mRNA expression in the liver of wild-type mice in LD had a circadian rhythm with a peak at ZT6 (Fig. 1A, left panel, 1-way ANOVA; $p < 0.05$) and a large oscillation amplitude (ca. 8-fold). In *Clock/Clock* mice, the mRNA levels significantly increased (2-way ANOVA; $p < 0.001$), and the pattern showed a significant rhythm (1-way ANOVA; $p < 0.05$), although the amplitude was lower (ca. 2-fold). *Cyp7a* expression in the liver of wild-type mice in DD also showed circadian rhythm with a delayed peak at CT10 (Fig. 1A, right panel, 1-way ANOVA; $p < 0.05$) with a 19-fold oscillation amplitude. In *Clock/Clock* mice, the mRNA levels significantly increased (2-way ANOVA; $p < 0.01$), and the pattern showed a rhythm (1-way ANOVA; $p < 0.05$), although the amplitude was lower (ca. 2.5-fold). Northern blot analysis results were essentially the same as those obtained by real-time RT-PCR analysis (data not shown) CYP7A protein level in hepatic microsomal fractions of wild-type mice in DD showed circadian rhythm with a peak at

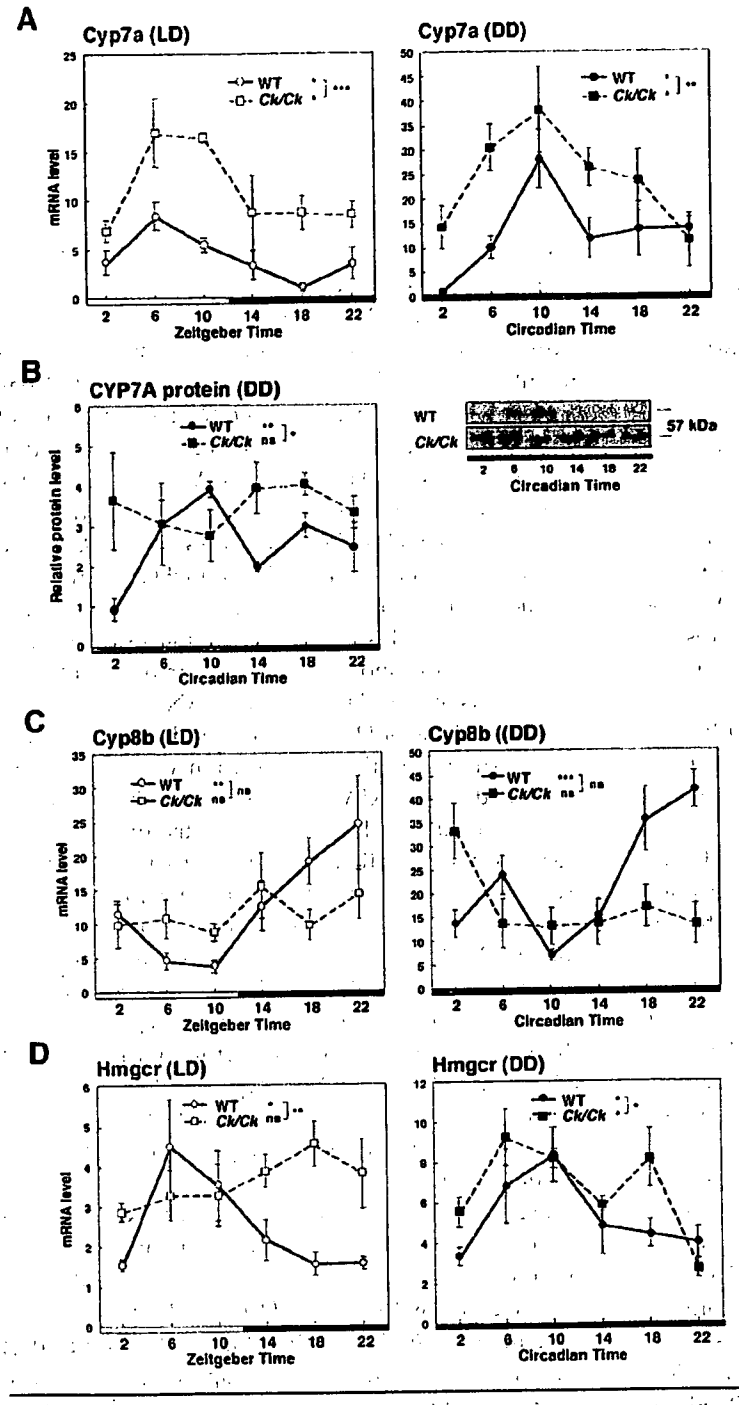

Figure 1. *Cyp7a* expression in the liver of wild-type and *Clock/Clock* mice. (A) *Cyp7a* mRNA levels were determined by quantitative real-time reverse-transcriptase PCR (RT-PCR). Data are plotted as mean ± SEM ($n = 4$). Open and closed bars for LD condition (left panel) indicate lights on and off, respectively, and gray bars indicate subjective day in DD condition (right panel). Time-series data were analyzed by 1-way analysis of variance (ANOVA) for rhythmicity (*$p < 0.05$; **$p < 0.01$; ***$p < 0.001$; *ns*, not significant). Differences between genotypes were tested by 2-way ANOVA. (B) Western blotting of CYP7A protein in the liver of DD condition. Quantitative data for 3 determinations are plotted as mean values ± SEM (left panel), and a representative photograph is shown (right panel). The size of CYP7A protein (57 kDa) is indicated. WT, wild-type mice; *Ck/Ck*, *Clock* mutant mice. Transcript levels of (C) *Cyp8b* and (D) *Hmgcr* were determined by quantitative real-time RT-PCR.

CT10 coincident to the peak of the *Cyp7a* transcript in the corresponding mice (Fig. 1A, right panel) with around a 4-fold amplitude. However, the expression pattern of CYP7A protein became arrhythmic in *Clock/Clock* mice at the same level as the peak in wild-type mice (Fig. 1B), which indicates that the lower amplitude (ca. 2.5-fold) of transcript rhythm was not reflected in its protein level.

For comparison, effects of *Clock* mutation on other hepatic oscillating genes, *Cyp8b* and *Hmgcr*, were examined. A marked circadian expression was observed on the transcript levels of *Cyp8b* in wild-type mice with peaks at ZT/CT22 (Fig. 1C), which were different from those of *Cyp7a* (Fig. 1A) and *Hmgcr* (Fig. 1D) as previously reported in rat liver (Ishida et al., 2000). *Clock* mutation abolished the circadian rhythm of *Cyp8b* in both LD and DD, but the average expression levels were almost the same as those of wild-type mice.

Expression profiles of *Hmgcr* in wild-type mice under LD and DD conditions showed strong circadian rhythm with peaks at ZT6 and CT10 (Fig. 1D), similar to those of *Cyp7a* as described (Jurevics et al., 2000; Oishi et al., 2005). *Clock* mutation abolished the circadian rhythm of *Hmgcr* in LD, but the average expression levels were almost the same as those of wild-type mice. Under DD condition, expression significantly increased and remained rhythmic with 2 peaks.

Multiple Regulators for Transcriptional Activities of the *Cyp7a* Gene

Numerous transcription factors—including DBP, LXRα, HNF4α, and LRH-1—are known to up-regulate the expression of *Cyp7a* (Chiang, 2002). To estimate the relative potency of various transcription factors for the regulation of *Cyp7a* expression—in addition to the known regulatory factors—other possible nuclear factors, such as REV-ERBα/β and RORα/β/γ—were examined by luciferase reporter assay in

HepC2 culture using rat *Cyp7a* promoter (−731 to +35), which contains potent response elements for DBP, LXRα, HNF4α, and LRH-1, previously identified (Lavery and Schibler, 1993; Lee et al., 1994; Lu et al., 2000; Chiang, 2002). Figure 2A shows dose-dependent enhancements of the *Cyp7a* promoter by various transactivators, which had plateau levels at 50 to 100 ng of the respective expression plasmids of DBP, LXRα, and LRH-1 or near-maximal levels at 100 to 200 ng for the respective expression plasmids of HNF4α and REV-ERBα/β. DBP most strongly activated the *Cyp7a* promoter (> 40-fold), and LXRα:RXRα heterodimer was also a potent activator for *Cyp7a* (ca. 7-fold), whereas LXRβ:RXRα heterodimer did not have any significant enhancement on the promoter activity (data not shown) (Peet et al., 1998). HNF4α showed 4-fold enhancement of the *Cyp7a* promoter activity, whereas LRH-1 showed only 1.4-fold enhancement at maximum. Interestingly, orphan nuclear receptors REV-ERBα and REV-ERBβ enhanced promoter activity (7- and 4-fold, respectively), whereas RORα had little effect on the promoter activity. Under similar experimental conditions, both REV-ERBα and REV-ERBβ repressed the RORα-activated reporter construct containing RRE of *Bmal1* (data not shown), as previously reported (Guillaumond et al., 2005).

Since previous studies had reported that PPARα, E4BP4, and DEC2 suppress the *Cyp7a* transcription (Patel et al., 2000; Noshiro et al., 2004), these factors were examined to determine whether they affect the *Cyp7a* promoter transactivated by the potent activators described above. Control activities in the absence of activators were only slightly suppressed by the addition of the expression plasmids for PPARα, E4BP4, and DEC2 (data not shown). *Cyp7a* promoter activities transactivated by DBP, LXRα:RXRα heterodimer, REV-ERBα, or HNF4α were suppressed by DEC2, E4BP4, or PPARα (Fig. 2B), and transactivation of the *Cyp7a* promoter by DBP was most sensitive to DEC2 suppression (Noshiro et al., 2004) (Fig. 2C). E4BP4 moderately suppressed all enhanced promoter activity, and PPARα significantly suppressed all enhanced promoter activity, although it was less effective on the enhanced activity by REV-ERBα. When all 4 activators (DBP, LXRα, REV-ERBα, and HNF4α) were combined, the enhanced level (ca. 48-fold) was close to that with DBP alone (ca. 44-fold), and suppression by DEC2, E4BP4, or PPARα was similar to that in the case of DBP alone.

Clock Mutation Abolished the Hepatic Expression of *Dbp*, *Dec2*, and *Rev-erbα/β* but Enhanced *E4bp4* Expression

Among the regulatory factors for *Cyp7a* described above, *Dbp*, *Dec2*, *Rev-erbα/β*, and *E4bp4* are known to exhibit marked circadian rhythm in normal animals (Preitner et al., 2002; Noshiro et al., 2004). Figure 3A shows that *Dbp* mRNA expression in the liver of wild-type mice had strong circadian rhythms with peaks at CT6 (1-way ANOVA, $p < 0.001$). In *Clock/Clock* mice, *Dbp* expression was almost completely abolished, as recently reported (Oishi et al., 2003; Noshiro et al., 2005). Similarly, expression profiles of *Dec2* in the liver of wild-type mice also showed a strong circadian rhythm with peaks at CT6 (Fig. 3B, 1-way ANOVA, $p < 0.001$), as reported (Noshiro et al., 2004, 2005). *Clock* mutation also completely abolished the expression of *Dec2*. The above results indicate that DBP and DEC2 do not contribute to the regulation of *Cyp7a* in *Clock/Clock* mice. Expression profiles of *Rev-erbα* in the liver of wild-type mice also showed a strong circadian rhythm with peaks at CT6 (Fig. 3C, 1-way ANOVA, $p < 0.01$), similar to those of *Dbp* and *Dec2*, and *Clock* mutation abolished the rhythmic expression of *Rev-erbα*. As described above, REV-ERBα enhances the transcription of *Cyp7a*, which shows the contribution of REV-ERBα to the circadian regulation of *Cyp7a*, to some extent, in normal state. However, the expression profiles of *Rev-erbα* in *Clock/Clock* mice indicate that REV-ERBα does not contribute to the circadian regulation of *Cyp7a* in *Clock/Clock* mice. Expression profiles of *Rev-erbβ* in the liver of wild-type mice also showed a strong circadian rhythm with peaks at CT10 (Fig. 3D, 1-way ANOVA, $p < 0.001$). *Clock* mutation diminished the expression level but had a significant rhythm (1-way ANOVA, $p < 0.01$), but with a lower amplitude.

Figure 3E shows that *E4bp4* mRNA expression in the liver of wild-type mice had a circadian rhythm with a peak at CT22 ($p < 0.01$), which is 180 degrees out of phase with that of *Dbp*, *Dec2*, and *Rev-erbα* (Mitsui et al., 2001; Noshiro et al., 2004), suggesting that the role of E4BP4 in the suppression of *Cyp7a* expression differs from that of DEC2 (Noshiro et al., 2004). In contrast to the expression profiles of *Dbp*, *Dec2*, and *Rev-erbα*, *E4bp4* in *Clock/Clock* mice was significantly enhanced ($p < 0.001$), especially in a subjective day, whereas the expression in wild-type mice was lower; this resulted in arrhythmicity at enhanced

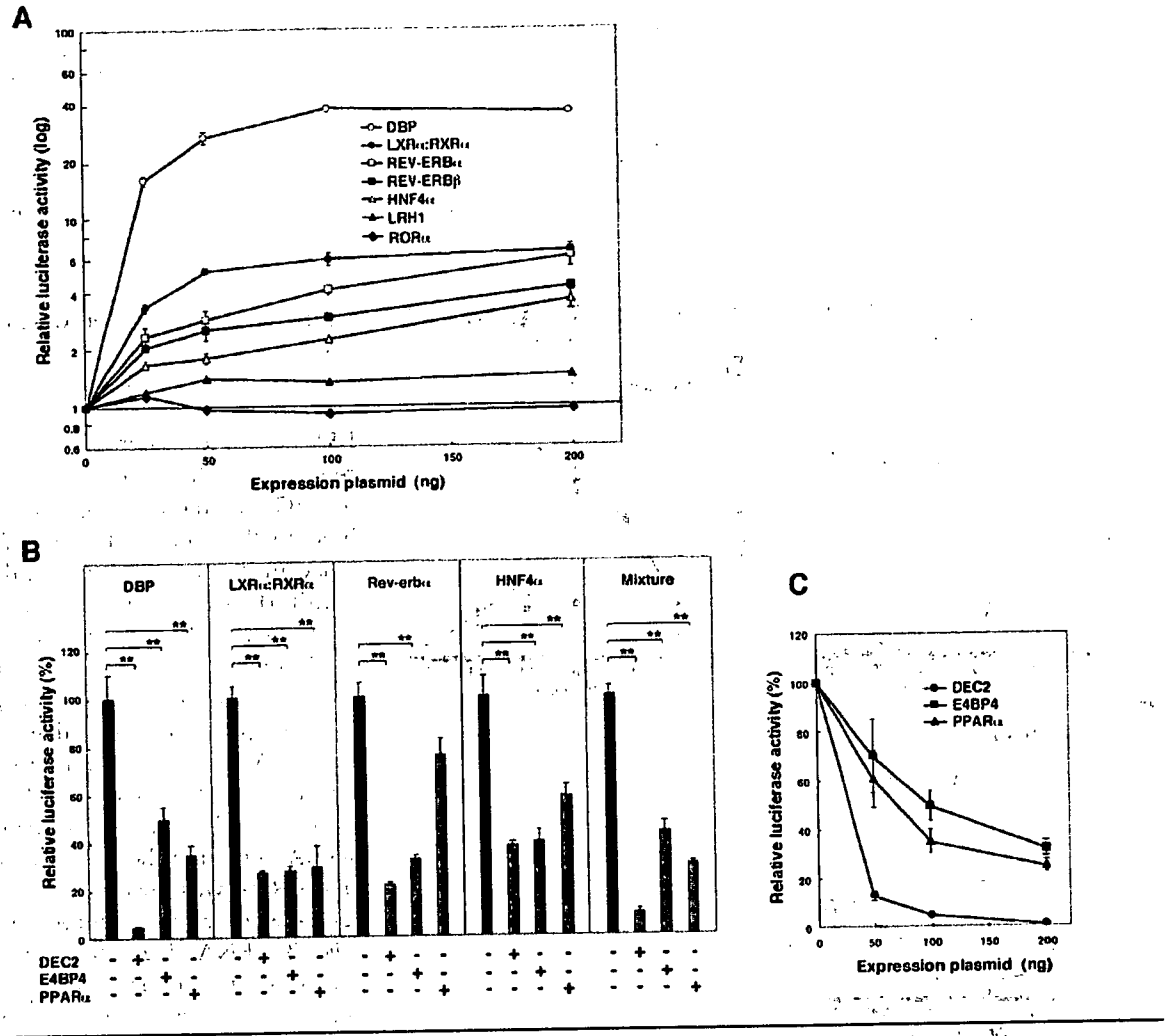

Figure 2. *Cyp7a* promoter activity is dose-dependently enhanced by various activators, and these enhanced activities are repressed by DEC2, E4BP4, and PPARα. (A) HepG2 cells in a 24-well plate were cotransfected with pCYP7A-Luc (−731 to +35, 20 ng/well), internal control pRL-TK (20 ng/well), and various expression plasmids for DBP, LXRα:RXRα, REV-ERBα, REV-ERBβ, RORα, HNF4α, and LRH-1 at concentrations of 25, 50, 100, and 200 ng/well. Data are expressed in a logarithmical scale. (B) Expression plasmids (100 ng/well) for DEC2, E4BP4, and PPARα were cotransfected with pCYP7A-Luc in the presence and absence of each activator (50 ng/well). When *Lxrα* and *Pparα* were used, T0901317 (10^{-7} M) and WY-14643 (10^{-5} M) as their respective agonists were added to the culture medium (Gottlicher et al., 1992; Willy et al., 1995). *Rxrα* was cotransfected when *Lxrα* and *Pparα* were used. The luciferase activities were normalized by *Renilla luciferase* activities of the internal control pRL-TK, and data are plotted as mean values ± SEM in triplicate assay. Data are shown as percentages of the luciferase activity enhanced by the respective activator plasmid. Significance of the difference between respective control and addition of each suppressor was analyzed by Student *t* test (**$p < 0.01$). All the experiments were repeated at least 3 times and yielded reproducible results. (C) The enhanced luciferase activity by DBP was dose-dependently suppressed by DEC2, E4BP4, and PPARα.

levels, which indicates that E4BP4 is involved in the regulation of *Cyp7a* in *Clock/Clock* mice.

Hepatic Expression of *Lxrα*, *Hnf4α*, and *Pparα* Was Maintained in *Clock* Mutant Mice

Hepatic expressions of *Lxrα* were arrhythmic in wild-type mice (Fig. 4A). In *Clock/Clock* mice, *Lxrα* expression levels increased at CT14 to CT18 but were not significantly rhythmic. LXRα protein levels in hepatic nuclear extracts of wild-type mice in DD showed an arrhythmic expression pattern (Fig. 4B), and there was no significant change in *Clock/Clock* mice.

Another activator for the *Cyp7a* gene, *Hnf4α*, showed higher expression at CT6 to CT10 in wild-type mice (Fig 4C), with a significant rhythm. In

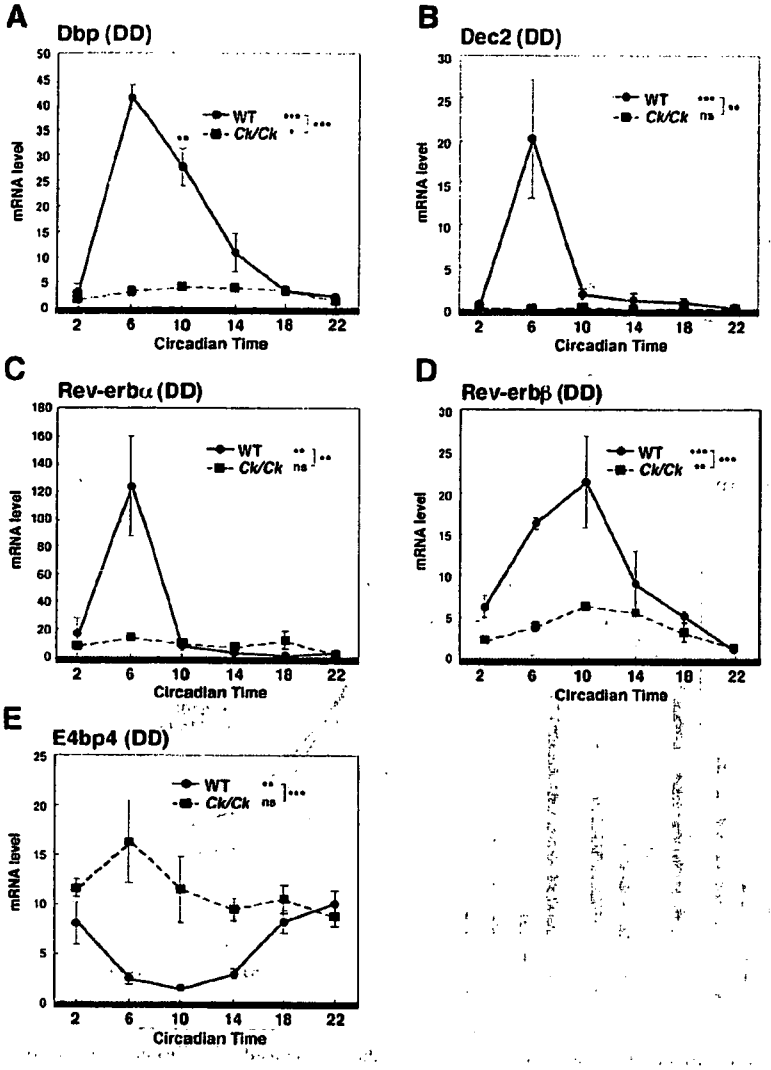

Figure 3. *Clock* mutation abolished the circadian expression of (A) *Dbp*, (B) *Dec2*, (C) *Rev-erbα*, and *Rev-erbβ* but enhanced *E4bp4* expression (E) in the liver. The mRNA levels were determined by quantitative real-time reverse transcriptase PCR (RT-PCR). Data are plotted as mean ± SEM ($n = 4$). Gray bars indicate subjective day in DD condition. Time-series data were analyzed by 1-way analysis of variance (ANOVA) for rhythmicity (*$p < 0.05$; **$p < 0.01$; ***$p < 0.001$; *ns*, not significant). Differences between genotypes were tested by 2-way ANOVA. WT, wild-type mice; *Ck/Ck*, *Clock* mutant mice.

Clock/Clock mice, the *Hnf4α* expression became arrhythmic, and the expression level was slightly but significantly increased ($p < 0.01$). Another known suppressor for *Cyp7a*, *Pparα*, had similar expression profiles to those of *Hnf4α* in the liver of wild-type mice (Fig. 4D, $p < 0.01$). In *Clock/Clock* mice, *Pparα* expressions in both light conditions were arrhythmic, but the average expression level was similar to that of wild-type mice. Taken together with the previous sections, these results suggest that LXRα, HNF4α, REV-ERBβ, E4BP4, and PPARα contribute to the regulation of expression of *Cyp7a* in *Clock/Clock* mice, where the most potent regulators for rhythmic expression of *Cyp7a*, such as DBP, DEC2, and REV-ERBα, are absent.

REB-ERBα/β Are Direct Activators for *Cyp7a*

The orphan nuclear receptors REV-ERBα/β generally act as a repressor in the molecular clock system (Guillaumond et al., 2005) and bind to the 5-bp A/T-rich sequence adjacent to an AGGTCA half site (RRE) (Harding and Lazar, 1993). Since REV-ERBα/β enhanced the *Cyp7a* promoter, however, to confirm the action of these nuclear receptors, *Rev-erbα/β* was down-regulated using siRNA. As shown in Figure 5A, transcript levels of *Rev-erbα* and *Rev-erbβ* were markedly reduced by respective siRNA, although the effect with *Rev-erbα* siRNA was lower. *Cyp7a* mRNA levels were partly reduced by *Rev-erbα/β* siRNA (Fig. 5B), suggesting that those factors are transactivators for *Cyp7a* in living cells. The partial suppression by these siRNA is attributed to the participation of multiple factors in the regulation of *Cyp7a*.

To further examine the interaction of REV-ERBα and REV-ERBβ in the promoter region of the *Cyp7a* gene, EMSA was performed. Several motifs similar to the AGGTCA half site—the nuclear receptor motif—were found in the 240-bp upstream region of the rat *Cyp7a* gene promoter, although the canonical RRE motif was not found. Oligonucleotides for this region were prepared (Fig. 6A) and used to examine their binding capacity to REV-ERBα and REV-ERBβ proteins. As shown in Figure 6B, faint but specific retarded bands were observed for probe 1 (–33 to –82) with either the REV-ERBα or REV-ERBβ protein, whereas neither RORα nor RORβ showed a retarded band. Probe 1 also

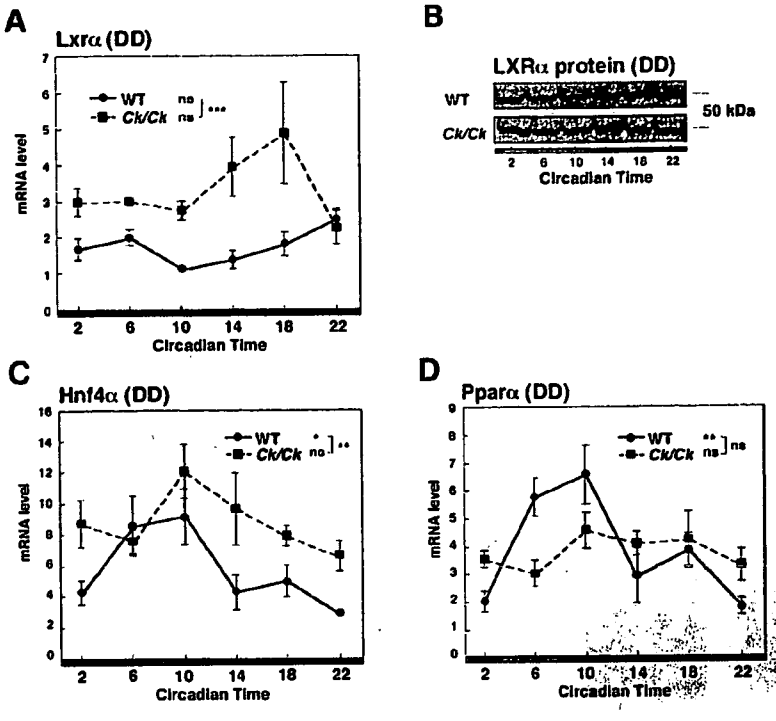

Figure 4. Effects of *Clock* mutation on the expressions of (A) *Lxrα* and (B) LXRα protein, (C) *Hnf4α*, and (D) *Pparα* in the liver. The mRNA levels were determined by quantitative real-time reverse-transcriptase PCR (RT-PCR). Symbols and other conditions are the same as those described in the legend to Figures 1 and 3. Western blotting of LXRα protein in the liver in the DD condition is shown (B). The size of the LXRα protein (50 kDa) is indicated.

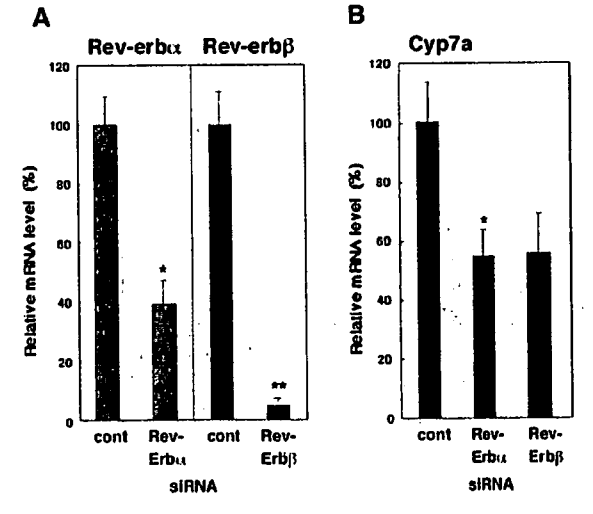

Figure 5. Effects on *Cyp7a* expression of knockdown of *Rev-erbα* and *Rev-erbβ* by siRNA. Transcript levels of (A) respective target genes and (B) *Cyp7a* were examined on the Hepa-1c1c7 transfected with siRNA for *Rev-erbα* or *Rev-erbβ*. $^{*}p < 0.05$. $^{**}p < 0.01$.

contains LXRE, which bound to the LXRα:RXRα heterodimer (Fig. 6B, right panel). Other DNA fragments (probes 2 and 3) did not show any retarded band with those nuclear receptors.

DISCUSSION

Bile acids are essential for the solubilization and absorption of lipids and lipid-soluble vitamins in the intestine, and they represent the major pathway for the metabolism and excretion of cholesterol in vertebrates. Cholesterol 7α-hydroxylase is a key enzyme for the biosynthesis of bile acids from cholesterol (Danielsson et al., 1967) and is known to exhibit a marked circadian rhythm in rodents (Myant and Mitropoulos, 1977; Noshiro et al., 1990). Transcription of the *Cyp7a* gene is now known to be regulated, directly or indirectly, by many transcription factors, including DBP, DEC2, E4BP4, LXRα, RXRα, HNF4α, LRH-1, PPARα, and FXR (Chiang, 2002; Noshiro et al., 2004). In addition, REV-ERBα and REV-ERBβ were found to up-regulate the *Cyp7a* gene in this study. DBP, DEC2, E4BP4, and REV-ERBα/β are thought to be involved in the circadian regulation of *Cyp7a* (Lavery and Schibler, 1993; Lee et al., 1994; Noshiro et al., 2004) since they exhibit a marked circadian rhythm (Wuarin and Schibler, 1990; Mitsui et al., 2001; Preitner et al., 2002; Noshiro et al., 2004). The present and previous studies demonstrate that hepatic DBP, DEC2, and REV-ERBα are the most potent regulators for the circadian regulation of *Cyp7a* and that they are dominantly regulated by the CLOCK:BMAL1 heterodimer (Ripperger et al., 2000; Preitner et al., 2002; Butler et al., 2004; Hamaguchi et al., 2004). Nevertheless, *Clock* mutation, which caused depletion of *Dbp*, *Dec2*, and *Rev-erbα*, did not abolish the circadian expression of the *Cyp7a* transcript, which indicates that other mechanisms support the rhythmic expression of *Cyp7a* as discussed below. The lower but remaining rhythm of the *Cyp7a* transcript in *Clock* mutant mice suggested that action of CLOCK on *Cyp7a* gene expression is apparently less predominant or indirect, although the putative consensus binding site (CACGTG E-box)

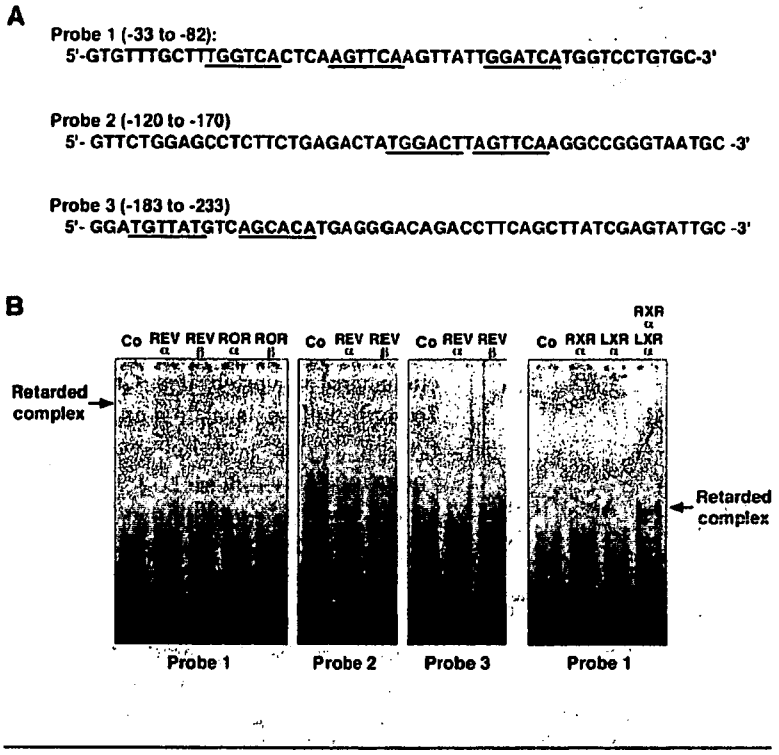

Figure 6. REV-ERBα and REV-ERBβ proteins bound to the proximal region of rat CYP7A gene promoter. (A) Double-stranded synthetic probes containing motifs similar to AGGTCA half-site were prepared. (B) Electrophoretic mobility shift assay (EMSA) was performed with ^{32}P-labeled double-stranded probes and the nuclear receptors. The radioactivities of retarded bands were visualized by the FLA-3000G fluoro-image analyzer (Fujifilm Co.).

for CLOCK:BMAL1 was found far upstream of the *Cyp7a* gene of the mouse (at –5.5 kb) by computer search (Panda et al., 2002). Whether this CACGTG E-box is functional for the CLOCK:BMAL1 heterodimer remains to be elucidated.

Based on the evaluation of the potency of various activators for *Cyp7a* promoter activity, DBP is the most potent, and LXRα, REV-ERBα/β, and HNF4α are moderate activators. The high potency of DBP is demonstrated by the existence of 4 D-boxes in the proximal region of the *Cyp7a* promoter (Lavery and Schibler, 1993; Lee et al., 1994). The enhanced *Cyp7a* promoter activities by those activators were more or less suppressed by DEC2, E4BP4, and PPARα. The sum of the contributions of these positive and negative factors, as well as others not described here, seems to constitute the circadian expression profiles of the *Cyp7a* transcript in a normal state (Fig. 7, upper panel), although the actual extent of the contributions of the respective factors in vivo is difficult to evaluate. In the liver of clock mutant mice, however, the circadian expressions of *Dbp*, *Dec2*, and *Rev-erbα* were almost completely abolished, as described above. Consequently, LXRα, REV-ERBβ, and HNF4α as activators, as well as E4BP4 and PPARα as suppressors, can support the expression of *Cyp7a* in the liver of clock mutant mice, which may cause the enhanced but less rhythmic expression of *Cyp7a* (Fig. 7, lower panel). The less rhythmic expression profiles of the *Cyp7a* transcript and CYP7A protein in *Clock* mutant mice indicate that DBP, REV-ERBα, and DEC2 are more important than other factors for the strong rhythm of *Cyp7a*. Moreover, in *Clock* mutant mice, the depletion of the most potent suppressor, DEC2, seems to be essential in increasing the expression level of the *Cyp7a* transcript despite the depletion of the potent activators DBP and REV-ERBα.

The orphan nuclear receptors REV-ERBα/β are important molecular components driving the antiphasic expression of the positive limb in the molecular circadian machinery (Preitner et al., 2002; Roenneberg and Merrow, 2003): Various studies have shown that REV-ERBα/β bind to 5-bp A/T-rich sequence adjacent to an AGGTCA half-site (RRE) (Harding and Lazar, 1993; Guillaumond et al., 2005) and generally act as a repressor (Forman et al., 1994), but 1 report differs (Harding and Lazar, 1993). However, the circadian expression profiles of these nuclear receptors, their enhancing activity for the *Cyp7a* promoter, suppression of *Cyp7a* expression with their siRNAs, and their binding to the proximal promoter region of the *Cyp7a* gene indicate that REV-ERBα and REV-ERBβ contribute to the circadian regulation of *Cyp7a* as activators (Fig. 7). RORα did not affect the *Cyp7a* promoter and did not bind to DNA fragments of the *Cyp7a* gene containing the REV-ERB-binding site (designated as RRE-like in Fig. 7), which indicates that the regulatory mechanism of REV-ERBα/β for *Cyp7a* is apparently different from that for other genes such as *Bmal1*, which is suppressed by REV-ERBα/β, especially when activated by RORα.

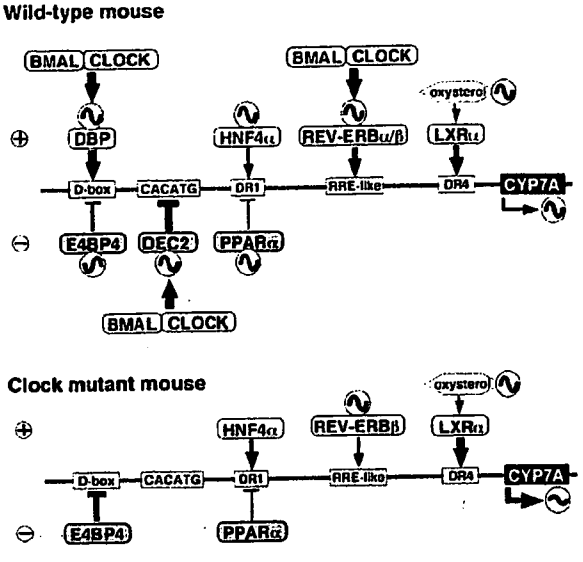

Figure 7. Regulation of rhythmic expression of the *CYP7A* gene in the liver. DBP, REV-ERBα/β, HNF4α, and LXRα enhance the expression of the *Cyp7a* gene, whereas DEC2, E4BP4, and PPARα suppress *Cyp7a* expression. E4BP4 antagonizes DBP action by binding to the DBP responsive element (D-box). Other factors bind to the respective response elements, although the precise binding site of REV-ERBα/β was not identified. Numbers and positions of each response element do not necessarily indicate actual ones. In clock mutant mice, DBP, REV-ERBα, and DEC2, which are dominantly regulated by the CLOCK:BMAL1 heterodimer through the CACGTG E-box, were abolished. In contrast, the expression of REV-ERBβ, LXRα, and E4BP4 remained and may maintain the rhythm of *Cyp7a* expression. The thickness of arrows indicates relative potential of each factor as an activator or suppressor based on activities in the reporter assays and their expression levels. RRE-like: assumed REV-ERB binding site; DR1: direct repeat of AGGTCA with 1-nucleotide space; DR4: direct repeat of AGGTCA with 4-nucleotide space.

Lxrα transcript and LXRα protein level did not demonstrate any significant circadian rhythm in the livers of wild-type mice or *Clock* mutant mice, which indicates that the circadian expression of the *Cyp7a* transcript is probably not related to the expression level of LXRα. On the other hand, LXRα is activated by oxysterols as ligands (Schroepfer, 2000) to mediate transactivation of *Cyp7a* by binding to an LXR regulatory element (LXRE) in the promoter (Willy et al., 1995; Janowski et al., 1996). Moreover, dietary or endogenous cholesterol is a source of oxysterols, and both feeding time and the biosynthetic phase of cholesterol, which is controlled by oscillating HMGCR, may produce a circadian rhythm of LXRα ligands. Dietary oxysterols are incorporated into plasma lipoproteins and the liver (Vine et al., 1998; Ando et al., 2002). Consequently, the activation of LXRα may contribute to a circadian regulation of *Cyp7a* irrespective of the expression profile of LXRα (Fig. 7).

Concerning the feeding time, another possible mechanism inducing the rhythm of *Cyp7a* in *Clock* mutant mice is a feedback regulation by bile acids via the FXR-SHP-LRH-1 pathway (Goodwin et al., 2000). In this pathway, FXR (NP1H4) is activated by bile acids and increases SHP (NR0B2), which interacts with the action of LRH-1 and eventually down-regulates *Cyp7a* transcription. Ligands for FXR—bile acids—are newly synthesized or supplied by entero-hepatic circulation and play a part in circadian phenomena. Although transactivation of the *Cyp7a* promoter by LRH-1 is much lower than other factors, as described previously (Lu et al., 2000) and confirmed in this study, contribution of this regulatory pathway to the circadian regulation of *Cyp7a* cannot be ruled out and needs to be evaluated in future work.

Another interesting finding concerning the phases of *Cyp7a*, *Cyp8b*, and *Hmgcr* showed different peak times of their expressions between mouse and rat: *Cyp7a* had peaks at ZT6 to ZT10 and ZT22, *Cyp8b* had peaks at ZT22 and ZT10, and *Hmgcr* had peaks at ZT6 and ZT18 in mouse and rat, respectively, according to the present study and our previous data (Noshiro et al., 2004). In contrast, the phases of clock-related genes in the SCN showed similar profiles between mouse and rat (Butler et al., 2004; Sato et al., 2004). These observations indicate species-dependent variations in circadian phases of peripheral gene expressions.

HNF4α and PPARα are known regulators of *Cyp7a* expression, being activator and repressor, respectively (Chiang, 2002), as confirmed in this study. The circadian expression of hepatic *Hnf4α* is reported for the first time in this study, whereas that of *Pparα* in mouse liver was reported previously (Patel et al., 2001). The expression profiles of both factors in the liver of wild-type mice are similar, and their expression levels are not significantly affected by *Clock* mutation, although rhythmicity did change. Consequently, HNF4α and PPARα, along with other factors, may contribute to the regulation of *Cyp7a* to some extent in wild-type mice, although the contribution of HNF4α and PPARα to the *Cyp7a* rhythm in *Clock* mutant mice appears to be much less.

In conclusion, the robust circadian expression of DBP and REV-ERBα/β (as positive regulators) and DEC2 and E4BP4 (as negative regulators) is necessary for the strong circadian expression of *Cyp7a*, but LXRα,